A THESIS SUBMITTED TO
THE GRADUATE SCHOOL OF NATURAL AND APPLIED SCIENCES
OF ÇANKIRI KARATEKİN UNIVERSITY

ENERGY AND EXERGY ANALYSIS OF A NAPTHA REFORMING PROCESS

IN PARTIAL FULFILLMENT OF THE REQUIREMENTS
FOR
THE DEGREE OF MASTER OF SCIENCE
IN
CHEMICAL ENGINEERING

BY

TAHA ASHEOOE ISSA ISSA

ÇANKIRI

2023

ENERGY AND EXERGY ANALYSIS OF A NAPTHA REFORMING PROCESS

By Taha Asheooe Issa ISSA

July 2023

We certify that we have read this thesis and that in our opinion it is fully adequate, in scope and in quality, as a thesis for the degree of Master of Science

Advisor **:** Assoc. Prof. Dr. Ömer Faruk DİLMAÇ

Examining Committee Members:

Chairman **:** Assoc. Prof. Dr. Korkut AÇIKALIN
Energy Systems Engineering
Yalova University

Member **:** Assoc. Prof. Dr. Barış ŞİMŞEK
Chemical Engineering
Çankırı Karatekin University

Member **:** Assoc. Prof. Dr. Ömer Faruk DİLMAÇ
Chemical Engineering
Çankırı Karatekin University

Approved for the Graduate School of Natural and Applied Sciences

Prof. Dr. Hamit ALYAR
Director of Graduate School

I hereby declare that all information in this document has been obtained and presented in accordance with academic rules and ethical conduct. I also declare that, as required by these rules and conduct, I have fully cited and referenced all material and results that are not original to this work.

Taha Asheooe Issa ISSA

ABSTRACT

ENERGY AND EXERGY ANALYSIS OF A NAPTHA REFORMING PROCESS

Taha Asheooe Issa ISSA

Master of Science in Chemical Engineering

Advisor: Assoc. Prof. Dr. Ömer Faruk DİLMAÇ

July 2023

Petroleum refining involves numerous physical separation and chemical conversion processes that have high energy consumption. The impact of global warming, one of today's most significant global issues, is increasing day by day. Therefore, it is becoming more important to enhance the energy efficiency of industrial facilities with high energy consumption and to carry out production with lower energy consumption by reducing energy losses. One of the most important tools used to improve the energy efficiency of thermal processes and reduce energy losses is energy and exergy analysis based on the second law of thermodynamics. In this study, the energy and exergy analysis of the naphtha reforming facility, where the octane number of products such as naphtha and gasoline is increased, located at the Salahuddin-1 Refinery in Baiji, Iraq, was conducted. The simulation of the facility under actual operating conditions was performed using the AVEVA Pro/II Process simulation program. In the simulation model, the hydrogen recycle flow rate fed to the catalytic naphtha reforming reactor was increased from 30,000 kg/h to 35,000 kg/h under real operating conditions. This proposed change resulted in a 2% increase in the energy efficiency of the reforming unit, a 1% increase in exergy efficiency, and a 0.71 MW decrease in exergy destruction.

2023, 66 pages

Keywords: Exergy analysis, Process simulation, Naphtha reforming

ÖZET

BİR NAFTA REFORMİNG PROSESİNİN ENERJİ VE EKSERJİ ANALİZİ

Taha Asheooe Issa ISSA

Kimya Mühendisliği, Yüksek Lisans

Tez Danışmanı: Doç. Dr. Ömer Faruk DİLMAÇ

Temmuz 2023

Petrol rafinasyonu enerji tüketiminin yüksek olduğu birçok fiziksel ayrıştırma ve kimyasal dönüştürme süreçlerini içermektedir. Günümüzde en önemli küresel sorunlardan biri olan küresel ısınmanın etkisi her geçen gün artmaktadır. Bu nedenle enerji tüketiminin fazla olduğu sanayi tesislerinin enerji verimliliğinin arttırılması ve enerji kayıplarının azaltılarak daha düşük miktarda enerji tüketilerek üretimin gerçekleştirilmesi önem kazanmaktadır. Termal proseslerin enerji verimliliğinin arttırılması ve enerji kayıplarının azaltılması amacıyla kullanılan en önemli araçlardan birisi termodinamiğin ikinci kanunu temelinde yapılan enerji ve ekserji analizleridir. Bu çalışmada, Salahuddin-1 Rafinerisi, Baiji, Irak'ta bulunan, nafta, benzin vb. ürünlerin oktan sayısının arttırıldığı nafta reformasyon tesisinin enerji ve ekserji analizi yapılmıştır. AVEVA Pro/II Proses simülasyon programı kullanılarak tesisin gerçek çalışma şartlarında benzetimi yapılmıştır. Simülasyon modeli üzerinde gerçek çalışma şartlarında katalitik nafta reforming reaktörüne beslenen hidrojenin geri döngü akış hızı 30.000 kg/h'ten 35.000 kg/h'e çıkarılmıştır. Önerilen bu değişiklik sonucunda reforming ünitesinin enerji veriminde %2, ekserji veriminde %1'lik artış, ekserji tahribi ise 0,71 MW azalma olduğu tespit edilmiştir.

2023, 66 sayfa

Anahtar Kelimeler: Ekserji analizi, Proses simülasyonu, Nafta reforming

PREFACE AND ACKNOWLEDGEMENTS

After a year of arduous work, I am finally happy to have ended this thesis. It was an amazing experience, and I will remember it for a long time.

I would like to thank my advisor Assoc. Prof. Dr. Ömer Faruk DİLMAÇ for their patience, guidance, and understanding.

Finally, I would like to express my endless thanks to my family, who always stood by me and encouraged me throughout my life, especially my parents, for whom I am grateful for their support, motivation, and encouragement to reach my goals and achievements.

Taha Asheooe Issa ISSA
Çankırı-2023

CONTENTS

LIST OF SYMBOLS

c_p	Specific heat (kJ/kg K)
$\dot{C}$	Exergy cost rate ($/h)
e	Specific exergy (MJ/kg)
e^{ch}	Specific chemical exergy (kJ/kg)
e^{ph}	Specific physical exergy (kJ/kg)
E	Energy (MW)
h	Specific enthalpy (kJ/kg)
h_o	Specific enthalpy at ambient conditions (kJ/kg)
H	Enthalpy (MW)
H_o	Enthalpy at ambient conditions (MW)
$\dot{I}_{pot}$	Improvement potential (MW)
k	k-th component
$\dot{m}$	Mass Flow Rate (kg/h)
P	Pressure (kPa)
P_0	Pressure at ambient conditions (kPa)
Q	Heat (W)
R	Gas constant (kJ/kmol K)
s	Specific entropy (kJ/kg k)
s_0	Specific entropy at ambient conditions (kJ/kg k)
S_{gen}	Specific entropy generated (kJ/kg K)
T	Temperature (K)
T_0	Ambient temperature (K)
w	Specific work transfer (J/kg)
W	Work (J)
$\dot{\Xi}$	Total Exergy (MW)
Ξ_R	Exergy rejected (MW)
Ξ^{ph}	Physical exergy (MW)
Ξ^{k}	Kinetic exergy (MW)
$\Xi_k{}^{ch}$	Chemical exergy of the k-th component (MW)
$\Xi_f{}^{ch}$	Chemical exergy of the Fuel (MW)
Ξ_L	Lost exergy, exergy loss (MW)
Ξ^{ch}	Chemical exergy (MW)
Ξ^{P}	Potential exergy (MW)
Ξ_D	Exergy destruction (MW)
Ξ_p	Exergy of product (MW)
Ξ_f	Exergy of fuel (MW)
ε	Exergetic efficiency
η	Energy efficiency

LIST OF ABBREVIATIONS

Act.	Actual
API	American Petroleum Institute
ASTM	American Society for Testing and Materials
CRF	Capital Recovery Factor
FG	Fuel Gas
HC-Gas	Hydrocarbon Gas
HHV	Higher Heating Value
HX	Heat Exchanger
LD	Light Distillate
Lig.	Liquid
OM	Operations and Maintenance
PFD	Process Flow Diagram
Prop.	Proposed
S	Stream
Sp.	Specific
TBP	True Boiling Point
tot	Total
Vap.	Vapour
wt.	Weight

LIST OF FIGURES

LIST OF TABLES

1. INTRODUCTION

Initially, thermal cracking processes were used, but in 1940 catalytic processes were introduced, which had a better yield and high octane. Still, they used molybdenum oxide as a catalyst after that. As a result of development and continuous studies in that period of the last century, they were changed to platinum.

Naphtha catalytic reforming is considered one of the most important in oil refineries and petrochemical industries (Figure 1.1). It works to improve the specifications of gasoline by enhancing the octane number of Heavy Naphtha from a low octane number in the range (30-60) to high octane number of gasoline normally (100), this doing by increasing aromatics and iso-paraffins content which it has a high-octane number.

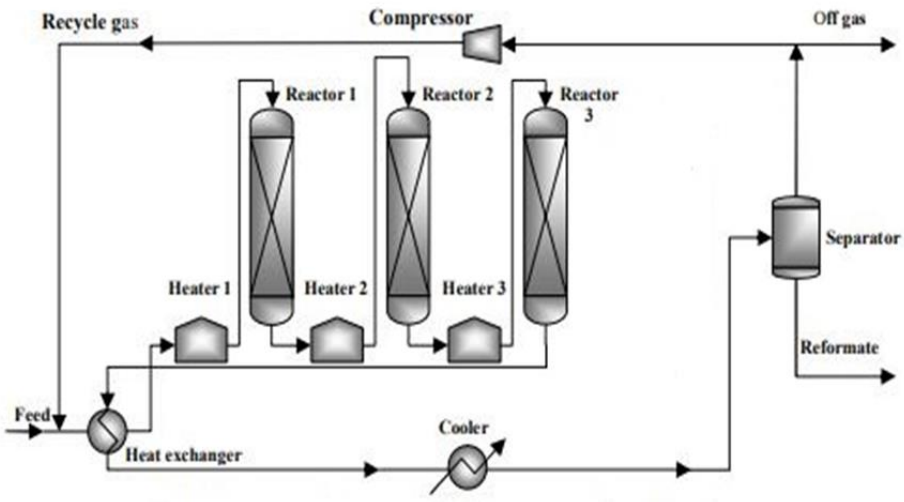

Figure 1.1 Naphtha catalytic reforming flow chart (Ancheyta-Juarez *et al.* 2001)

1.1 Heavy Naphtha

Hydrocarbon compounds are the main components of crude oil and its derivatives; heavy naphtha is the first crude oil derivative from the top of the distillation tower and has high volatility and a low initial boiling point. Heavy Naphtha is complex in composition because it consists of groups of different hydrocarbon compounds, which are Paraffins, Naphthene, and aromatics) and the numbers of these compounds are in the hundreds

(Antos and Aitani 2004). Heavy Naphtha represents between (15 – 30 wt. %) of crude oil with a distillation range of (90-200°C) by using ASTM D86; all these characteristics depend on the specifications and quality of crude oil.

In the modern petrochemical industry: The process in which low octane number of naphtha feedstock is converted into high octane reformate product (benzene, toluene, and xylenes) is called catalytic reforming naphtha, another main byproduct which result from this process is hydrogen which has very uses such as: hydro treating, and hydrocracking (Antos *et al.* 1995).

The first usage of this process was in 1947 over the catalysts of platinum, the used catalysts developed in recent catalytic reforming units which included Gama alumina with metals, like: rhenium, platinum, and a little additive, like chlorine, Gasoline to be used as engine spirit. Naphtha can be a fraction of light naphtha with a boiling point ranging from 30°C to 90°C (Antos and Aitani 2004, Antos *et al.* 1995).

A portion of this heavy cut that boils below 150°C and contains mostly hydrocarbons [Before repair, is processed in unit Hydrotherapy, Reformation is a form of reaction in which the components of paraffin's, naphthenic, and aromatics are rearranged to produce higher gasoline.

There are seven types of reactions in the catalytic naphtha reforming: dehydrogenation - isomerization - cyclization - aromatization - hydrocracking - hydrogenolysis - coke Formation (Ancheyta-Juarez *et al.* 2001).

Typically, on 40–70% wt. paraffin, 20–50 wt.% naphthenic, 5–20 wt.% aromatic, Some of these reactions are desired like cyclization and aromatization because of increasing octane number of gas oil and some of them are undesired according to octane number and coke formation like: coke deposition and formation (Antos *et al.* 1995)

1.2 Research Objective and Problem Statement

The naphtha catalytic reforming plant can process 38,796 kg/hr of benzine (alternatively 75% vol. Benzine, 25% vol. Naphtha) feed. The primary product of the unit is stabilized reformate, which must meet the following specifications: a minimum RON (Octane Number) of 95 and a maximum of 1% wt. for C_4 and lighter components. However, during operation, the stabilized reformate product does not always meet these specifications, and the energy consumption tends to be unstable and occasionally high (Gary *et al.* 2019).

The primary objectives of this study are to achieve the necessary product specifications with minimal energy consumption, thereby reducing costs, by modifying the conditions of the actual process and analyzing the impact of these modifications on the resulting octane number. AVEVA PRO/II Simulation enhances plant performance through advanced process design, operational analysis, and engineering studies. It is engineered to conduct precise heat and material balance calculations for diverse chemical processes and provides an extensive selection of thermodynamic models applicable to nearly every industry (Ghasem 2021).

We utilized AVEVA PRO/II software, a leading simulator in the petrochemical industry, to replicate the real plant and examine the impact of process variable changes on product specifications. This allowed us to identify the optimal conditions that ensure the plant's stability and flexibility for future operations. The steps to achieve these objectives are outlined as follows:

1- Analysis and simulate the naphtha catalytic reforming plant of the Salahuddin-1 Refinery from Bai Hassan Crude oil.
2- Validate the developed simulation data with the raw data obtained from the operation manual of the catalytic reforming unit in Salahuddin-1 Refinery.
3- Analysis the effect of each parameter on octane number.
4- Set the optimum operation conditions based on the analysis of each parameter.
5- Obtain the optimum operation conduction by using the optimizer tool.

6- Investigate how to reduce fuel consumption in furnaces and calculate and compare exergy destructions and exergy efficiencies.

Based on the study of each parameter and the optimum operation conditions, suggest appropriate changes to obtain the best efficiency (Rahimpour *et al*. 2013). The information study is expected to allow operating personnel through the appropriate procedure for the naphtha reformer process to have a maximum octane conversion ratio of more than 95 percent of production (Gaggioli 1983)

2. LITERATURE REVIEW

Many researchers and interested people have studied the reformation of naphtha because of its great impact in the fields of large industry, and the biggest challenge was to obtain high-octane gasoline.

In their research, they used many programs to simulate the treatment process, and among the world-famous programs are AVEVA PRO/II. They conducted simulations either to develop the existing treatment process or for other cases, all to achieve the requirements of gasoline in terms of the octane number and the amount of undesirable light compounds and finding the appropriate operational conditions that guarantee at the same time the minimum required consumption of energy.

In 1959, first kinetic model for catalytic reforming was proposed by Smith (Smith 1959). Where he assumed that naphtha consists of paraffin, naphthene, and aromatics and in addition, it included hydrogen, ethane, propane, and butane and the number of reactions group are 10. The proposed mathematical model is suitable to study the effect of the reactors feed temperature, total pressure, and hydrogen to hydrocarbon feed ratio on the reformate compositions. The calculated reformate composition agrees very well with experimental plant data. Three process variables were studied as their effects on the reformate composition as follow.

- Increasing the reactors feed temperature will increase aromatic yield, which reach maximum values at 540 °C.
- Increasing the total pressure had a little effect on the decreasing the aromatics composition in the reformate.
- Increasing H_2/HC ratio had a little effect on the increasing aromatics composition in the reformate (Smith 1959).

Marin and Froment (1989) stated that if naphtha from C5 to C10 then the reactions series consist of 23 components, Taskar and Riggs (1997) developed Foment model which

included of 35 pseudo components in the reaction series (36 reactions). Zakari *et al.* (2019) studied the catalytic naphtha reforming process of Kaduna refining and petrochemical company using PROMs software, and the behavior of the concentrations of the paraffin, naphthene's and aromatics components along the reactor height and, the temperature profile of the reactors., they found increasing in research octane number (RON) was from the first to the fourth reactor due to increase in aromatization.

Mesa Gómez *et al.* (2016) studied the increase in naphtha production from a gas processing plant by simulating the existing plant using ASPEN HYSYS V7.3. It was mentioned that the naphtha production was increased to 99.13% after it was 82.79%, and the quality of the produced naphtha increased by 20.85%, all by adjusting the operational conditions of the process and modifying some Existing devices (Mesa Gómez *et al*. 2016).

Mohaddecy *et al*. (2006) studied the effect of catalyst distribution in reactors on the octane and octane barrel in the catalytic reforming unit of Tehran refinery and they simulated the current process by ASPEN HYSYS by using pilot data and found that the distribution of catalyst should be varied from 20, 30 and 50 percent to 17,5, 27,8 and 54,6 percent respectively , The proposed distribution will increase the octane number and octane barrel values to 0,8 and 0,2 percent respectively whilst the total mass of the catalyst and other operating conditions were kept constant (Mohaddecy *et al*. 2006).

Vashishtha *et al.* (2013) studied naphtha reforming using the ASPEN PLUS platform under the operating conditions They developed whole process flowsheet and changed temperature and hydrogen to feed ratio and found its effect on the aromatics and lower hydrocarbons present in the gasoline. The best operating condition which will get best high-octane number gasoline component at temperature of 550 °C and the H_2/HC feed ratio 0.67 (Vashishtha *et al.* 2013).

The suggested mathematical model can be used to investigate how the feed temperature, total reactor pressure, and hydrogen to hydrocarbon ratio affect the compositions of reformates. The estimated reformate content and experimental plant have excellent agreement (Liang *et al*. 2005).

S.Reza Seif Mohaddecy and others, The hydro treated HSRG enters the semi-regenerative reforming reactors, which are made up of three radial flow fixed bed reactors *(*Mohaddecy *et al*. 2006).

Analyzed naphtha catalytic reforming unit with four reactors and proposed physical model to describe the catalytic reforming radial flow reactor all the kinetics and thermodynamics equations are defined to describe the naphtha catalytic reforming reactions characteristics according to idealizing the complex naphtha mixture by representing paraffin, naphthene, and aromatic groups by single compounds. The simulation results agree well with actual operation unit data (Wu *et al*. 2011).

Figure 2.1 shows a naphtha reforming simulation using computer simulation program blocks (Wu *et al.* 2011).

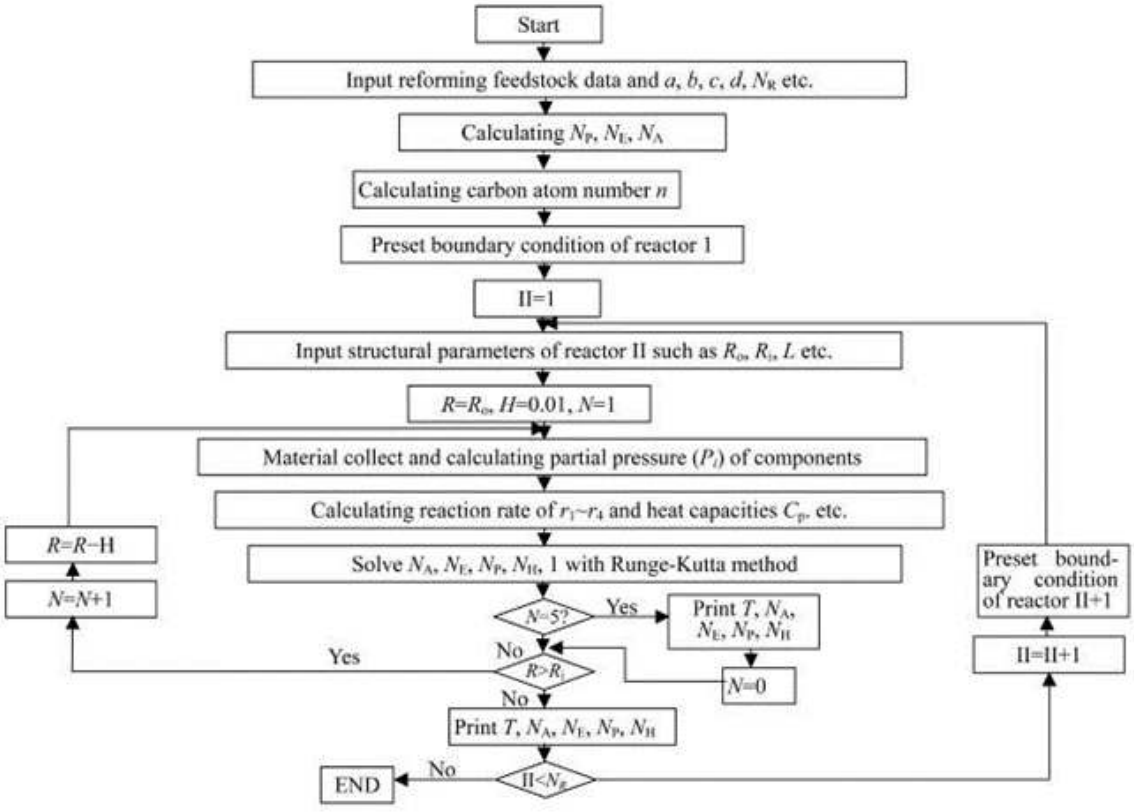

Figure 2.1 Naphtha reforming simulation flow chart (Wu *et al.* 2011)

Zaidoon M. Shakoor have studied the effect of parameters in Al-Doura catalytic naphtha reforming unit on the octane number of reformate by using Matlab software and he found the best conditions which will give aromatics composition in reformate from 63.42 % in actual unit to 70.89 % and this parameter as following: temperature 450°C to 520°C; total pressure 5 to 35 bar; H_2/HC feed ratio 3 to 8 (Shakoor 2013).

2.1 The Effecting Parameters on Naphtha Reforming

There are many factors that affect the process of reforming naphtha, and many researchers have studied them, and the following are the most important factors and conditions studied.

2.1.1 Pressure effect

Zaidoon M. Shakoor stated that increasing the pressure does not change the reformate composition seriously. Increasing the pressure has a small effect on decreasing of aromatics and hydrogen content in reformate, because the dehydrogenation of naphthene's and dehydrocyclization of paraffin’s and reducing hydrocracking favored lower (Shakoor 2013).

2.1.2 Effect H_2/HC ratio

Shakoor (2013) stated that the H_2/HC ratio has little effect on the aromatics yield, while reducing H_2/HC ratio is useful in reducing energy costs for corresponding and circulating hydrogen and favors the dehydrogenation of naphthenes and dehydrocyclization of paraffins. Unfortunately reducing H_2/HC ratio can also increase catalyst coking and decrease catalyst activity and increase hydrocracking reaction (Shakoor 2013).

Vashishtha *et al.* (2013) stated that when the feed flow rate ranges from 29,605 to 40,000 kg/hr, the composition of aromatics and lower hydrocarbons in the reformate increases with the feed ratio at a constant reactor temperature of 470°F (Vashishtha *et al.* 2013).

2.1.3 Reactor's inlet temperature effect

Askari *et al.* (2012) and others stated that no effects on octane number when inlet temperature of reactors in range 495-505°C. Shubhi Vashishtha and others stated that when feed flow rate constant of 30410 kg/hr., and when reactor temperature change in range 350°C to 550°C, it was observed that as the temperature increases, the composition of aromatics in the gasoline also increases (Askari *et al.* 2012).

3. MATERIALS AND METHODS

The primary objective of catalytic reforming is to transform low-octane hydrocarbons into hydrocarbons with elevated octane numbers. Reforming is a catalytic process involving the rearrangement of paraffins, naphthenes, and aromatics to enhance gasoline quality. In catalytic naphtha reforming, there are seven primary reaction types:

1. Dehydrogenation
2. Isomerization
3. Cyclization
4. Aromatization
5. Hydrocracking
6. Hydrogenolysis
7. Coke Formation

Each reaction plays a critical role in optimizing the composition of the final product. Certain reactions, such as cyclization and aromatization, are favorable due to their contribution to increasing the octane number of gas oil. Conversely, other reactions are undesirable with respect to octane number enhancement and coke formation, including coke deposition and formation.

3.1 Process Description

A brief introduction of the Naphtha Catalytic Reforming unit at the Salahuddin Refinery, which will undergo simulation followed by energy and exergy analysis, is presented along with the process design and operational details. The process flow diagram is provided in Figure 3.1.

Before feeding naphtha into the catalytic reforming unit, it typically undergoes heavy naphtha hydrotreating to eliminate impurities. This step is crucial to ensure that the hydrotreated naphtha is suitable for introduction into the catalytic reformer. The platinum-based catalyst used in the reformer is highly sensitive to poisoning by these

impurities, making their removal essential. The reformer feed pump (401 J) is employed for delivering naphtha into the system, where it is combined with circulating gas. This mixture then passes through heat exchangers 401 C and 402 C, followed by the initial section of heater 401 B, prior to entering reactor 401 D.

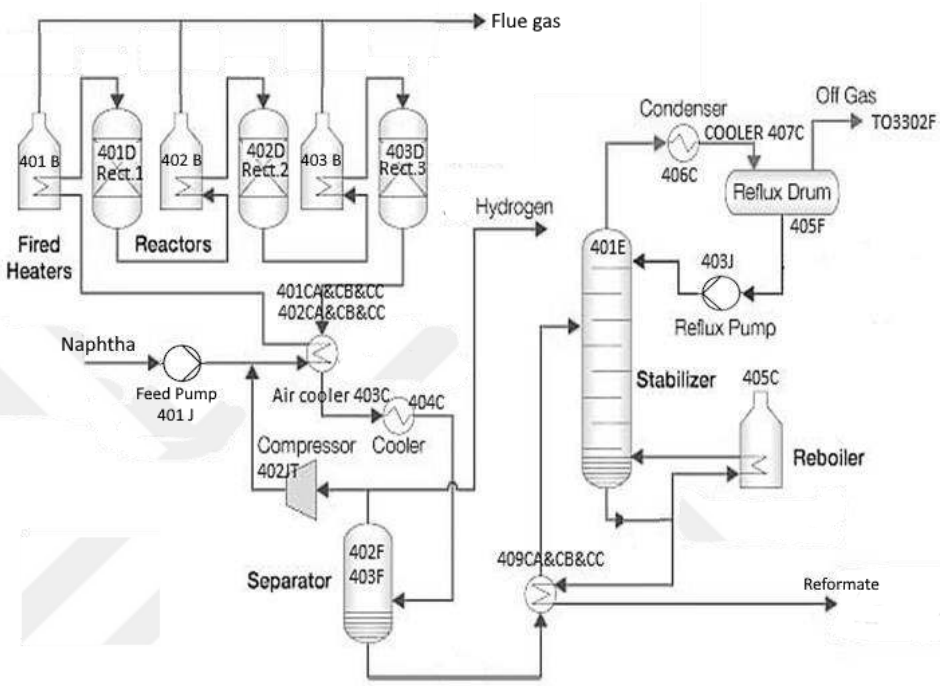

Figure 3.1 Process Flow Diagram (PFD) of naphtha reforming unit

Where; D reactor, B heater, F drum or tank, J pump, JAT turbine pump, C heat exchanger or air cooler, E stabilizer tower, 3302 - Light distillate HDS unit.

Due to the predominance of endothermal reactions, the mixture undergoes heating, necessitating preheating in subsequent sections of heater 401B to achieve the requisite temperature for reactors 402D and 403D. The mixture from the reactor elevates the temperature of reboiler 405°C, with heat exchange occurring in exchangers 401C and 402C to regulate the incoming mixture's temperature. Following cooling in air coolers 403C and 404C, the mixture enters separator 402F, facilitating the separation of liquid and gas phases. Gas containing hydrogen passes through knockout drum 403F and is recirculated into the system via compressor 402JT, while excess hydrogen is directed to unit 3302 - Light Distillate HDS Unit. In the event of HDS unit shutdown, gas may be

directed to the fuel gas system. Compressor 404J may route hydrogen gas to hydrogen storage drums 404FA, B, C, D, where it is stored at 19.6 MPa pressure to support unit start-up operations. After further heating in heat exchanger 409C, liquid from the separator is directed to stabilizer 401E. Vapors from the stabilizer top go through the air cooler 406 C and condenser 407 C into the reflux drum 405 F. After cooling the stabilized reformate is pumped into storage tanks 2105 FA, B in unit 4502; in case of non-standard product, the reformate is discharged into the slop. The effluent gases originating from the reflux drum are routed into the fuel gas system. These gases serve as blanketing agents within the reforming unit and the storage drums for feedstock in the light distillate hydrodesulfurization (HDS) unit.

Reformer heater 401 B is provided in the convention section with 3,2 MPa, 410° C steam generation. Boiler feed water is discharged from utility block to the steam generator 407 F. Centrifugal pump 406 J, JAT pumps the water to the convection section of heater 401 B. Steam—water mixture is discharged into the steam generator 407 F, where the steam is separated end discharged to the steam preheater in heater 401 B. Pumps 405 J could charge propylendichloride end carbon desulphated into reactors 401 D, 402 D, 403 D.

3.2 Equipment Summary Sheets

It's very important to define the properties of all used equipment in real plant because there tell us about the boundaries which we can study and change in the process to obtain the maximum values of desired products. Table 3.1 provides data pertaining to vessels, reactors, and columns.

Table 3.1 Equipment summary data of vessels and reactors

Item	Service	Volume (m^3)	Diameter (m)	Length (m)	Max. Operating	
					Temper ℃	Disch.pres. Bar g
401 D	Reactor 1	10,5 (4,7)	2,4	2,91	530	36,3
402 D	Reactor 2	15 (9,5)	2,4	3,98	530	36,3
403 D	Reactor 3	24,5 (18,9)	2,4	6,09	530	36,3
401 F	Charge Drum	28,8	2,4	6,9	60	2,3
402 F	Separator	36	2,4	9,04	43	31,4
403 F	K.O Drum	10,7	1,6	5,94	43	31,4
405 F	Reflux Drum	5	1,4	3,5	43	22,7
407 F	Steam Generator	5	1,6	3,28	241	36,8
408 F	Condensate Drum	11,5	2,0	3,9	95	atm
409 F	K.O. Facilities Pot	0,3	0,5	1,65	100	7,8
410 F	Blowdown Cooler	0,2	0,45	1,46	100	atm
404 F	H_2 Storage Drums	4*14	1,4	14,9	86	212,8
411 F	Condensate Drum	10,6	1,6	5,74	240	1,0
401 E	Stabilizer	-	1.8/1.2	20+10 trays	85-252	22.7

3.3 Process Variables

Main purpose for catalytic reforming is to convert low octane hydrocarbons into hydrocarbons with higher octane number. These chemical transformations occur on a platinum-rhenium (Pt-Re) catalyst in the presence of hydrogen under specified conditions. Among the various reactions involved, the fundamental ones are as follows (Equation (3.1) – Equation (3.4)):

naphthene's dehydrogenation:

$$N \rightarrow A + H_2 \quad (3.1)$$

paraffin’s isomerization:

$$np \rightarrow A + H_2 \quad (3.2)$$

paraffin’s dehydrocyclization:

$$(i+n)p \rightarrow A + H_2 \quad (3.3)$$

paraffin’s hydrocracking:

$$(i+n)p + H_2 \rightarrow \text{Lower hydrocarbons} \quad (3.4)$$

Where; N; naphtha, n; normal, p; paraffin’s, i; iso paraffin

These reactions are subject to the principles of kinetics and thermodynamics, dictating their progression towards thermodynamic equilibrium via variations in reaction rates. Achieving optimal equilibrium is contingent upon process parameters, with reaction kinetics, facilitating equilibrium attainment, primarily contingent upon the quality and properties of the catalyst (Liang *et al.* 2005).

Operating conditions are very important for the process design as well as for whole operation. The primary process variables include: Reactor Inlet Temperature, Reactor Pressure, Circulating Gas to Feed Ratio, and Space Velocity. The operating conditions for the catalytic naphtha reforming process are presented in Table 3.2.

Table 3.2 Operation condition of naphtha reforming process

ITEMS	unit	Values
Inlet temperature of reactors	^{o}C	500
Outlet temperature	^{o}C	491
Liquid space velocity in reactor bed	-	1.6
Catalyst volume	m^3	33.1
Feed stock ratio H_2/HC	Nm^3/m^3	1600
Type of Catalyst		Pt – Re
Benzine from distillation temperature	^{o}C	60
Benzine from storage tanks temperature	^{o}C	43
Reformate temperature	^{o}C	43
Hydrogen gas temperature	^{o}C	88
Hydrocarbon gas temperature	^{o}C	43
Pressure on third reactor outlet	barg	36.4

Increasing reactor inlet temperature results in operating security. Hydrocracking reactions are more sensible to temperature raise than aromatization reactions. Coke deposits are a function of temperature raising as well. Optima temperature, though, at reactor inlet is kept as low es possible to obtain the octane number required.

Pressure decreasing results more in aromatization reactions and at the same time limits hydrocracking. Therefore, the lower pressure results in higher yields of reformate and hydrogen and decreases the quantity of gaseous products. On the other side the lower pressure results in faster catalyst deactivation, because at lower hydrogen partial pressure coke deposits are higher and such deactivation could be compensated by circulation ratio increasing.

Circulating ratio is defined as a ratio of circulating gas quantity to feed quantity (sometimes also as a molar ratio of H_2 versus hydrocarbons). Circulating gas is used mainly for decreasing coke deposits on catalyst. Otherwise, over the pertinent minimum, circulating ratio influences the reaction only a little.

The space velocity LHSV (Liquid Hourly Space Velocity) is quantified as the quotient of the liquid feed's hourly flow rate and the volume of catalyst, serving as a metric for the operational intensity as expressed in Equation (3.5).

$$\text{LHSV}=\frac{\text{hourly feed flow rate at } 15°\text{C}/\text{m}^3/\text{h}}{\text{total volume of catalyst}/\text{m}^3} \quad (3.5)$$

If space velocity reduced and the feed flow rate reduced the hydrocracking reactions is favored but has practically no influence the aromatization reaction. Thus, a reduction or the space velocity at a constant temperature increases the octane number and reduces the yields. Hence the most important process variable is the temperature, which could be changed during operation at the easiest way, whilst the other variables has been practically fixed as early as at unit design.

3.4 Feedstock and Product Specification

The characteristics of the feedstocks utilized in the catalytic naphtha reforming unit are provided in Table 3.3, Table 3.4 and Table 3.5. Some of the presented data stem from laboratory analyses of the feedstocks employed in the unit, while others are sourced from design documents.

Table 3.3 Specification of Heavy Naphtha

Main design feedstock charge	Benzine
Mass flow rate of feed (kg/hr)	38796
Alternative charge	75% vol. Benzine, 25% Vol. Naphtha

Table 3.4 Analysis of the Bai Hassan crude oil using DHA (PIONA)

No.	**Component Name**	**Weight%**	**Vol%**
1	Pentane	0.850	0.962
2	2-methylpentane	3.363	3.650
3	3-methylpentane	3.610	3.854
4	Hexane	10.074	10.836
5	Methyl cyclopentane	2.259	2.139
6	Cyclohexane	1.741	1.587
7	2-methylhexane	3.995	4.180
8	1,1-dimethylcyclopentae	1.451	1.270
9	Heptane	5.441	5.607
10	Methylcyclohexane	1.199	1.132
11	Heptane	13.791	14.307
12	Methylcyclohexane	3.562	3.306
13	Toluene	3.504	2.861
14	2-methylheptane	4.303	4.366
15	4-methylheptane	1.338	1.325
16	3-methylheptane	3.475	3.495
17	Octane	10.958	11.066
18	1,1,4-trimethylcyclohexane	1.246	1.123
19	2,5-dimethylheptane	2.100	2.103
20	p-xylene	2.149	1.771
21	4-methyloctane	1.540	1.517
22	2-methyloctane	1.682	1.673
23	3-methyloctane	2.430	2.393
24	1,1,2-Trimethylcyclohexane	1.636	1.592
25	Nonane	8.218	8.128
26	1,2,4-Trimethylbenzene	1.417	1.163
27	Decan	2.669	2.595
	Sum:	100.000	100.000

Table 3.5 The specifications of benzine (gasoline) and naphtha derived from crude oil produced in the Bai Hassan oil field

ITEMS	Benzine	Naphtha
TBP cut °C	84-145	145-175
PONA % Vol. P	67.6	61.5
N	22.0	23.0
A	10.4	15.5
Specific gravity	0.732	0.773
Sulphur content ppm	<1	<1

Allowed deviations in PONA analysis: Paraffin's +2-1 %, Naphthene's:proportional, Aromatase: proportional.

Main unit product is stabilized reformate with following specification:
RON -min. 95, Butanes and lighter - max. 1. % wt.

Units shall be processed with higher butane content to achieve motor fuel specifications. The auxiliary product is hydrogen gas, with hydrogen content in the range of 66.9 - 54.6 % vol.

3.5 Simulation of Naphtha Reforming Unit

Simulating the catalytic naphtha reforming unit using AVEVA Pro/II is a pivotal step in optimizing refinery operations and enhancing process efficiency. The catalytic reforming process is fundamental in refining low-octane naphtha into high-octane gasoline components and valuable aromatics, as well as generating hydrogen as a by-product. By leveraging AVEVA Pro/II, a powerful process simulation software, engineers can model, analyze, and optimize this complex chemical process with high precision.

In this simulation study, we aim to replicate the operational conditions of the catalytic naphtha reforming unit at Salahuddin Refinery-1. Through detailed modeling, we will explore key aspects such as reaction kinetics, catalyst performance, energy requirements, and product distribution. The simulation provides invaluable insights into the unit's

behavior under various operating scenarios, facilitating informed decision-making for process improvements, troubleshooting, and strategic planning.

By utilizing AVEVA Pro/II's advanced simulation capabilities, this study seeks to enhance the understanding of the catalytic reforming process, identify opportunities for efficiency gains, and ensure optimal performance of the reforming unit within the refinery's integrated operations. Developing a simulation model for the catalytic naphtha reforming process, a crucial aspect of oil refining, is a highly complex and challenging task. The catalytic reformer model encompasses the feed characterization system, heat exchanger network, reactor section, stabilizer, and additional equipment. Figure 3.2 illustrates the block flow diagram, detailing key components of the naphtha reforming process, including catalytic reactors, heaters, and separation units. The reactor model is built upon rigorous kinetics. The feed characterization system are designed to work together with the refining assay system so the reformer model can be simulated in a refinery-wide flowsheet.

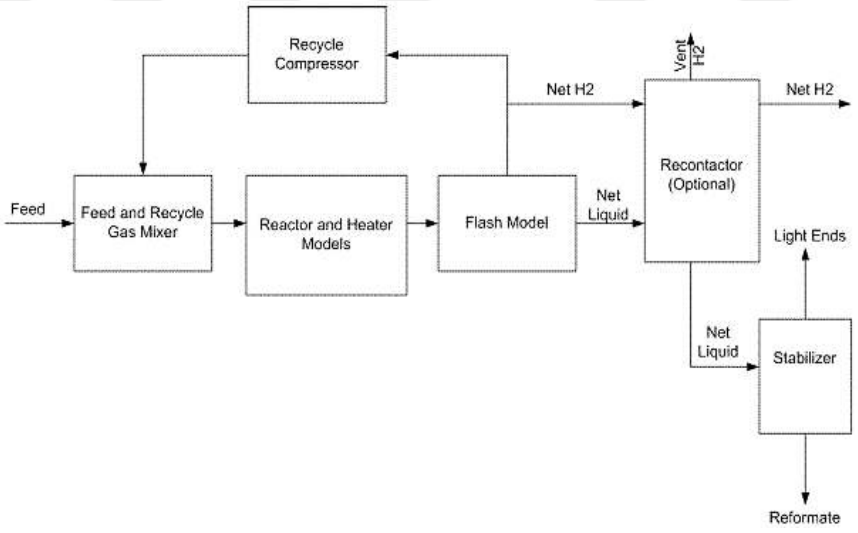

Figure 3.2 The Catalytic reformer block diagram

3.5.1 Simulation of the catalytic naphtha reformer

The catalytic naphtha reforming unit in the Salahuddin Refinery-1 is designed to convert low-octane naphtha into high-octane reformate, which is a valuable component for

blending high-quality gasoline. The process also produces hydrogen as a by-product, which can be utilized in other refinery operations.

In this research, we aim to achieve the following specifications; a Research Octane Number (RON) of at least 95, and a maximum of 1% by weight of C4 and lighter compounds.

Simulating naphtha reforming using AVEVA PRO/II is challenging, requiring precision and complexity. Accurate simulation demands comprehensive information, which we gather from both real plant data and the AVEVA PRO/II library specific to this process. Additionally, numerous steps are involved in completing the simulation accurately.

The simulation study concludes upon verification of the obtained data against the desired outcomes. If the desired results are not met, the process data is re-evaluated, prompting necessary adjustments for subsequent simulation runs. Selecting appropriate thermodynamic equations of state tailored to the chemical properties used in the process is crucial to ensure the accuracy of simulation results and the intended functionality of the system.

Simulation output data can be generated either manually as a consolidated report covering the entire process or automatically as individual reports for each device, typically in the form of Microsoft Excel files.

In this study, the Peng-Robinson equation of state was chosen to describe thermodynamic properties. Subsequently, a comprehensive system check was conducted, followed by running the simulation model. Figure 3.3 illustrates the Process Flow Diagram (PFD) of the naphtha reforming unit developed under operating conditions for this study.

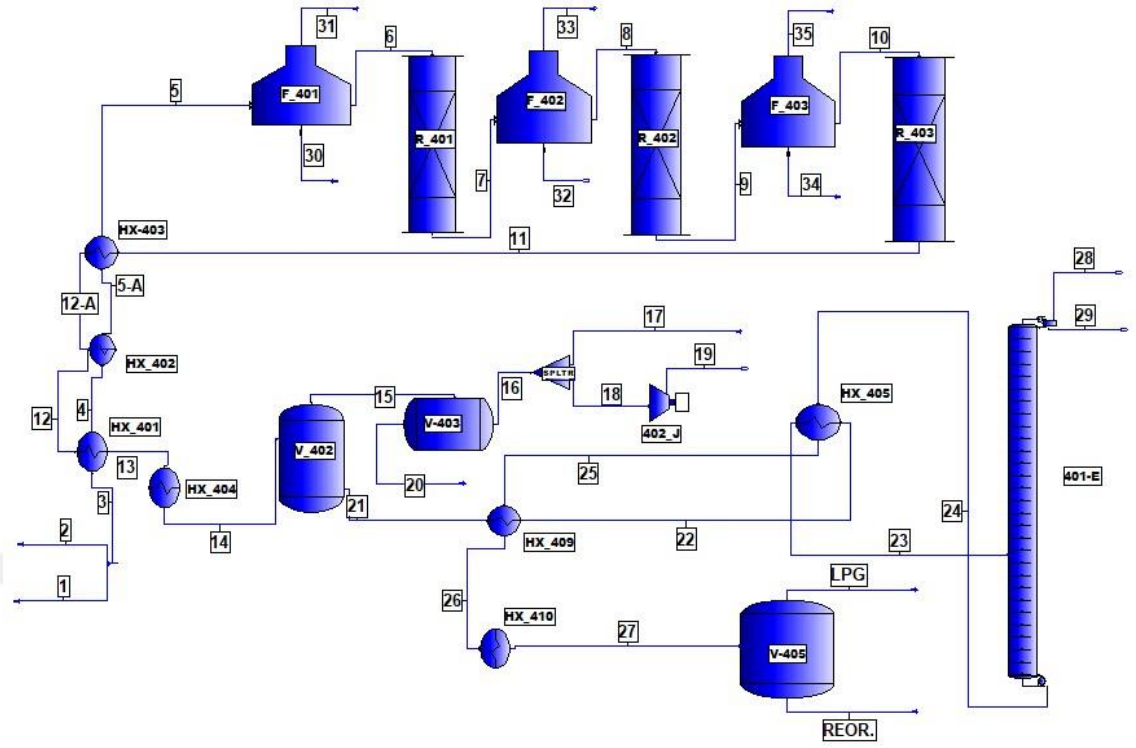

Figure 3.3 Naphtha reforming unit simulation PFD for real operation conditions

3.5.2 Define the blend of oil and choose the fluid package

Figures 3.4 illustrate defining a feedstock stream (Naptha reforming unit feed) based on petroleum assay data.

3.5.3 Simulation reactors and building models

We built the most important items in our simulation which are the reactors, we took into consideration the following issues (Table 3.6):

- Configuration data, such as like number of reactor beds, the reaction bed path lengths, and the catalyst inventory of each bed.
- Catalyst deactivation type, that is, semi-regen or CCR.
- Fresh feed rate.

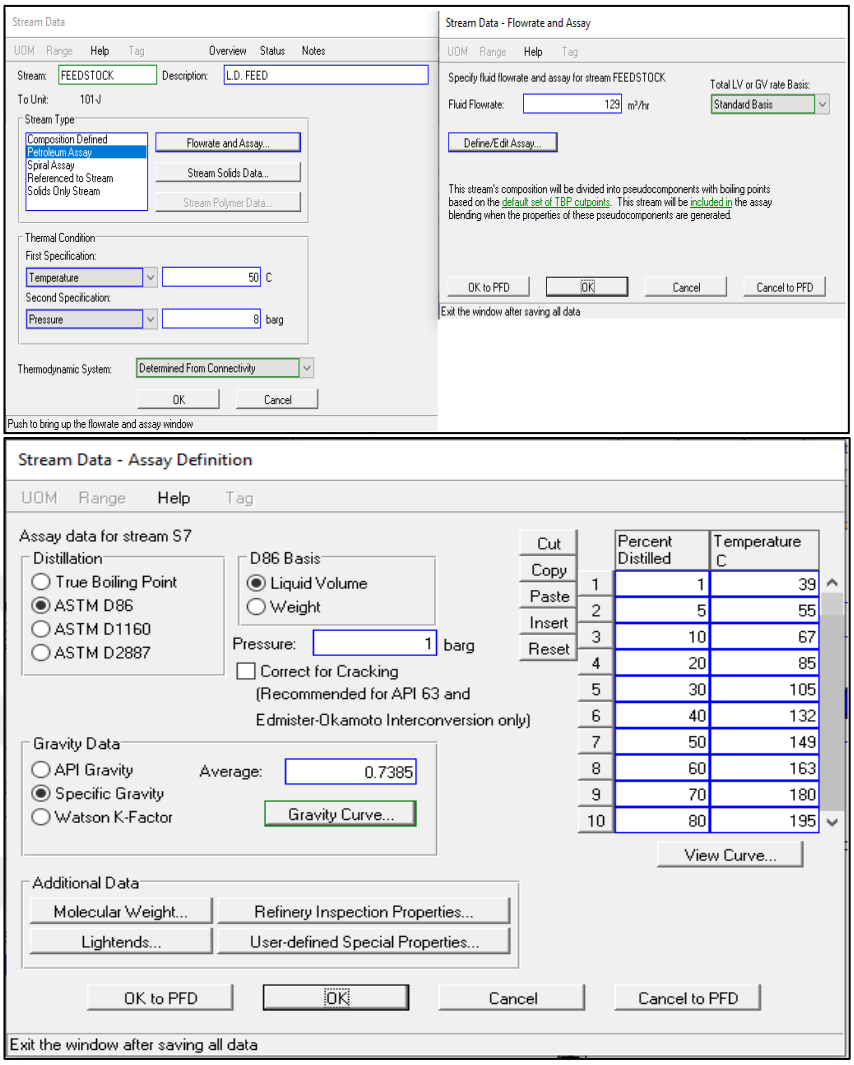

Figure 3.4 Petroleum assay-based feedstock definition window

- Reactor bed inlet temperatures (or WAIT, RON, or aromatics target with inlet temperature biases).
- Reactor bed inlet pressures.
- Recycle gas rate to first reactor bed and to other beds (if present).
- Product Separator T and P.
- Catalyst Rate for CCR as well as coke on catalyst for last reactor.
- Coke on catalyst at start of time period, start time, and end time for semi-regen configuration.
- Recontact or drum temperatures and pressures for systems with reconductors.
- Kinetic coefficients as determined from a calibration run.
- İsomerization tuning factors (for mapping a8, p4, and p5 lumps to molecules).

- Ethylbenzene isomerization factor, meta xylene isomerization factor
- Orth xylene isomerization factor, ic4 isomerization, ic5 isomerization

- Olefin distribution factor (to map paraffins to olefins to match olefin targets)
  - Ethylene isomerization factor, propylene isomerization factor
  - Butylene isomerization factor, pentene isomerization factor
  - Hexene isomerization factor, heptane isomerization factor
  - Octene isomerization factor
- Equilibrium constant tuning factors
  - C5 cyclization, c6 multi-branch isomerization
  - C7 multi-branch isomerization, c8 multi-branch isomerization
  - C6 single-branch isomerization, c7 single-branch isomerization
  - C8 single-branch isomerization
- Light ends tuning factors (factors for tune c1 through c4 product distribution)
- Kinetic pathways tuning factors (multipliers are reaction rates)
  - Dehydrogenation, hydrocracking, multi-branch isomerization
  - Single-branch isomerization, ring closure, ring expansion
- Dehydrogenation tuning factors by carbon number C7 and C8.

Table 3.6 The petroleum assay as inputs for the feed stream simulation model

Density	**kg/m^3**	657.717
Distillation Type		TBP
0%	**°C**	28.78
5%	**°C**	29.64
10%	**°C**	29.98
30%	**°C**	30.71
50%	**°C**	59.15
70%	**°C**	64.54
90%	**°C**	95.06
95%	**°C**	107.13
100%	**°C**	169.93
Composition Basis	**°C**	Volume %
Normal Paraffins	**vol %**	19.40
Isoparaffins	**vol %**	71.28
Olefins	**vol %**	0.00
Naphthenes	**vol %**	7.50
Aromatics	**vol %**	1.82

Next step: define the catalysts loading like reaction path length and catalyst weight and this information as shown in Table 3.7.

Table 3.7 Catalysts loading of reactors

	Bed 1	**Bed 2**	**Bed 3**	**Total**
Reaction Path Length [m]	2.9	3.94	6.09	
Catalyst Weight [kg]	6500	11500	27000	45000
Catalyst Distribution [%]	14.45	25.56	60	100
Catalyst Volume [m^3]	11.61	20.54	48.22	80.36
Catalyst Loaded Volume [m^3]	29.02	51.34	120.54	200.89

Now we must go to the reactor control section and enter reference temperature bias [^oC] as given in the previous, H_2/HC ratio - mole/mole as 1.60, product separator temperature as 28°C, product separator pressure 3500 kPa, product heater temperature 522°C and pressure 2840 kPa.

3.6 Results Simulation of Naphtha Reforming Unit

3.6.1 Reactors and heaters simulation result

The results of reactor simulation like conditions, residence time, Liquid Hourly Space Velocity (LHSV) and weight hourly space velocity (WHSV) are shown in Table 3.8.

Table 3.8 Results of Reactors Simulation

Items	**R-401**	**R-402**	**R-403**
Inlet Temperature [^oC]	500	500	500
Delta T [^oC]	455.27	480.89	491.53
Inlet Pressure [kPa]	101.73	61.11	34.47
Outlet Pressure [kPa]	763.10	676.32	627.52
Delta P [kPa]	70.79	57.75	41.17
Inlet Molar Flow [kgmole/h]	692.31	618.57	586.34
Outlet Molar Flow [kgmole/h]	1254.89	1523.12	1709.26
Residence Time [seconds]	1522.99	1709.14	1832.48
LHSV	0.862		
WHSV	0.862		

Heater simulation results are shown in Table 3.9.

Table 3.9 Fired Heaters simulation results

F-401 Heater Fired Duty [kJ/h]	27328679
F-402 Interheater Fired Duty [kJ/h]	26579009
F-403 Interheater Fired Duty [kJ/h]	16201643
Total Fired Duty [kJ/h]	70109332
Charge Heater Absorbed Duty [kJ/h]	17763642
Rx 2 Interheater Absorbed Duty [kJ/h]	17276356
Rx 3 Interheater Absorbed Duty [kJ/h]	10531068
Total Absorbed Duty [kJ/h]	45571066

From above results of reactors simulation, we could summaries them in Table 3.10 like Recycle H_2, H_2 Yield, Yields/RON, and Aromatic yields.

Table 3.10 summary results of reactors simulation

Recycle H2		
Recycle H2 Rate (_m^3/h)	30000	
Recycle H2 Purity	0.71	
H2 Yield		
H2 Yield, Wt. (%)	2.61	
Net H2 Rate (m^3/h)	15402.56	
H2 Production (m^3/m^3)	289.67	
H2 Purity, mole fraction	0.71	
H2/HC Ratio	1.6	
Yields/RON		
C5+ Yield, wt. (%)	85.37	
C5+ Yield, vol (%)	80.39	
C5+ RON	98.53	
C6+ Yield, wt. (%)	80.24	
C6+ Yield, vol (%)	74.60	
C6+ RON	100.36	
Reformate Production (m^3/h)	39.71	
Reformate RON	99.67	
Aromatic yields		
Items	Wt.%	Vol%
Benzene	17.51	14.42
Toluene	12.06	10.07
Ethyl-Benzene	2.01	1.68

Table 3.10 summary results of reactors simulation (Continued)

Para-xylene	1.64	1.38
Ortho-xylene	2.81	2.31
Meta-xylene	4.69	3.92
Total Xylenes	9.13	7.61
Total Aromatics	49.43	41.11

3.7 Exergy Analysis

Exergy investigations often aim to determine energy efficiency ratios as well as performance measurements for energy destruction and loss. Additionally, an exergy analysis is used to identify the true thermodynamic inefficiencies inside the energy conversion system.

In general forms like mass, energy, and entropy, exergy is an extensive property, so it too can be transferred into or out of a control volume where streams of matter enter and exit. Accordingly, the counterpart of Equation (3.6) applicable to control volumes requires the addition of terms accounting for such exergy transfers:

$$\underbrace{d\,\Xi_{cv}/dt}_{\text{rate of exergy change}}=\underbrace{\sum\left(1-\frac{To}{Tj}\right)Qj-(Wcv-po\frac{dVcv}{dt})+\sum(miEi)-\sum(meEe)}_{\text{rates of exergy transfer}}-\underbrace{\Xi D}_{\text{rate of exergy destruction}} \quad (3.6)$$

As for control volume rate balances considered in Chapter 2, the subscripts i and e denote inlets and outlets, respectively. In Equation (3.6), the term dE_{cv}/dt represents the time rate of change in the exergy of the control volume. The term Qj represents the time rate of heat transfer at the location on the boundary of the control volume where the instantaneous temperature is q, and the associated exergy transfer is given by.

$E_{q,j}=(1-\frac{To}{Tj}).Q_j$ (3.7)

As in the control volume energy rate balance, W_{cv} represents the time rate of energy transfer by work other than flow work. The associated exergy transfer is given by

$E_w=W_{cv}-P_o(d\,\Xi_{cv}/dt)$ (3.8)

where (dV_{cv}/dt) is the time rate of change of volume of the control volume itself. The term $m_i.e_i$ accounts for the time rate of exergy transfer at the inlet i. Similarly, m_ee_e accounts for the time rate of exergy transfer at the outlet e. In subsequent discussions, the exergy transfer rates at control volume inlets and outlets are denoted, respectively, as $Ei = m_ie_i$ and $Ee = m_ee_e$. Finally, E_D accounts for the time rate of exergy destruction due to irreversibilities within the control volume, $E_D = T_oS_{gen.}$

Steady-State Form. Since the engineering analyses considered in this book involve control volumes at steady state, it is important to identify the steadystate form of the exergy rate balance. Thus, by applying the steady-state conditions (dEcv/dt = 0 and dVcv/dt = 0), Equation (3.6) simplifies to Equation (3.9).

$0=\sum\left(1-\frac{To}{Tj}\right)Qj-(W_{cv}-P_0\frac{dVcv}{dt})+\sum(m_ie_i)-\sum(m_ee_e)-\Xi_D$ (3.9)

This equation states that the rate at which exergy is transferred into the control volume must exceed the rate at which exergy is transferred out; the difference is the rate at which exergy is destroyed within the control volume due to irreversibilities. Expressed in terms of the time rates of exergy transfer and destruction, Equation (3.8) takes the form.

$0=\sum(E_{q,j})-W_{cv}+\sum(E_i-E_e)-E_D$ (3.10)

where E_i and E_e are exergy transfer rates at inlets and outlets, respectively, and $E_{q,j}$, is given by Equation (3.7). For the thermodynamic analysis of control volumes at steady

state, Equations (3.9) for exergy may be added to the steady-state forms of the mass, energy.

The main components of exergy in a substance or stream include chemical exergy, physical exergy, potential exergy, and kinetic exergy.

$$\Xi = \Xi^{ch} + \Xi^{ph} + \Xi^{p} + \Xi^{k} \quad (3.11)$$

Potential energy and kinetic energy can be considered negligible because the system is in a stable equilibrium with its surroundings.

$$\Xi = \Xi^{ch} + \Xi^{ph} \quad (3.12)$$

$$\Xi^{ph} = \dot{m}.(h - h_o) - T_o.\ \dot{m}.\ (s - s_o) \quad (3.13)$$

$$\Xi^{ph} = (H - H_o) - T_o(S - S_o) \quad (3.14)$$

$$e^{-ch} = \sum x_k\, e_k^{-ch} + RT_o.\sum x_k \ln x_k \quad (3.15)$$

$\dot{m}$ (kg/h) represents the mass flow of the stream; T_o (K) and P_o (kPa) are the reference conditions temperature and pressure. Ξ_k^{ch} and y_k are the chemical exergy and proportion of the k-th component.

The Higher Heatin g Values (HHV) of petroleum derivatives and fuel mixtures are used to calculate their chemical exergy. Equation is used to compute chemical exergy.

$$\Xi^{ch} = \Delta H - T_0 \Delta S \quad (3.16)$$

If only the higher heating value were known, Equation (3.7) could calculate the fuel's exergy value:

$$\Xi^{ch} = -0{,}975 \Delta h_{combustion} \quad (3.17)$$

Equation describes the relationship between chemical exergy and fuels with higher heating values Equation (3.8).

$$e_F^{ch}/\,HHV = \begin{cases} 0.95 - 0.985 & \text{for gas fuels } (CH_4 \text{ and } H_2 \text{ not including}) \\ 0.98 - 1 & \text{for liquid fuels} \\ 1.00 - 1.04 & \text{for solid fuels} \end{cases} \quad (3.18)$$

Equation (3.19) gives the proportion of chemical energy to fuels with higher heating values (HHV).

$$HHV = -\,\Delta H^{*} = 17672 + 66{,}6\,G - 0{,}316\,G^2 - 0{,}0014\,G^3 \quad (3.19)$$

Here, ΔH^{*} is the Gross Calorific Value of oil fractions, and G the API gravity.
The sum of the exergy leaving a thermal system and the exergy lost must always equal the exergy entering the system.

$$\Xi_{in} = \Xi_{out} + \Xi_L \quad (3.20)$$

In the system, the exergy lost can be calculated by the equation:

$$\Xi_L = \Xi_D + \Xi_R \quad (3.21)$$

Here, (Ξ_L) is the total loss exergy, (Ξ_D) destroyed exergy resulting from irreversibility (entropy production) in the system, and (Ξ_R) is the exergy rejected out by the release of heat to the environment with exergetic waste material flows.

The system is zero, the Ξ_D due to irreversibility can be found from the difference between the Ξ_{in} entering the system and the Ξ_{out} leaving the system.

$$\Xi_D = \Xi_{in} - \Xi_{out} = T_o S_{gen} \quad (3.22)$$

In this study, $\Xi_{D,k}$ is the exergy destruction for the k-th system component. Then, only the $\Xi_{L,tot}$ is defined for the whole system. For component k, an exergy balance equation can

be written in a general form. And for the entire system, the exergy balances are given below, respectively:

$$\Xi_{F,k} = \Xi_{P,k} + \Xi_{D,k} + \Xi_{R,k} \quad (3.23)$$

$$\sum \Xi_F \sum \Xi_P + \sum \Xi_D + \sum \Xi_R \quad (3.24)$$

Where the exergy of product is ($\Xi_{P,k}$) and the exergy of fuel is ($\Xi_{F,k}$).

The ($\Xi_{L,k}$) for the k-th is zero when the boundaries are drawn at the surrounding temperature T_o.

($\Xi_{D,k}$) can be written as follows:

$$\Xi_{D,k} = T_o S_{gen,k} \quad (3.25)$$

The exergy balance for the whole system is:

$$\Xi_{F,tot} = \Xi_{P,tot} + \Xi_{D,tot} + \Xi_{L,tot} \quad (3.26)$$

Where $\Xi_{D,tot}$ is equal to $\sum_k \Xi_{D,k}$

The ratio between the $\Xi_{P,k}$ and $\Xi_{F,k}$ is the exergetic efficiency for the component k:

$$\varepsilon_k = \Xi_{P,k} / \Xi_{F,k} = 1 - (\Xi_{D,k} / \Xi_{F,k}) \quad (3.27)$$

Moreover, for the overall system:

$$\varepsilon_{tot} = \Xi_{P,tot} / \Xi_{F,tot} = 1 - ((\Xi_{D,tot} + \Xi_{L,tot}) / \Xi_{F,tot}) \quad (3.28)$$

The summation of exergy destructions of the components is the ($\Xi_{D,\,tot}$)

$$\Xi_{D,tot} = \sum \Xi_{D,k} \quad (3.29)$$

Calculating the irreversibility caused by D can be done using the difference between the exergy entering and exiting the system if the exergy rejected out of the system is zero.

$$\dot{I}_{pot} = \sum \Xi_D (1 - \varepsilon) \quad (3.30)$$

4. RESULTS AND DISCUSSION

4.1 Exergy Analysis Calculations

This section presents the exergy analysis results derived from the simulation model data under both current and proposed operational conditions, as discussed in the third section. Additionally, it includes the equations used for the energy and exergy analysis of the naphtha reformer unit.

T_o = 298.15 K and P_o = 101.325 kPa are the accepted reference environment conditions for calculations in the energy and exergy study. Kinetic and potential energy changes are not considered in the exergy analysis for the reformer unit. Equation (3.4) was used to determine the feed and product streams' **physical exergy**. Equations (3.8) and (3.9) were also used to compute the **chemical exergies** (Tsatsaronis 2008).

The energy and exergy balances for the primary components of the naphtha reformer unit including reactors, the stabilizer column, heat exchangers, the compressor, and heating furnaces were each analyzed separately.

4.2 Energy and Exergy Analysis of the Reactors

Balance Equations for the catalytic Reactors in the naphtha reformer unit are (Figure 4.1, Table 4.1):

Mass balance:

$$\dot{m}_6 = \dot{m}_7 \quad (4.1)$$

Energy Balance:

$$E_6 = E_7 \quad (4.2)$$

Energy efficiency:

$$\eta = (E_7)/(E_6) \quad (4.3)$$

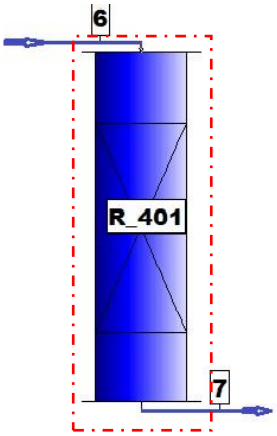

Figure 4.1 System boundary of the reactor

The exergy equation is written based on Equation (3.13) as follows:

$$\sum \Xi_P = \dot{m}_7 (e_7^{ch} - e_6^{ch}) + \dot{m}_7 (e_7^{ph} - e_6^{ph}) \quad (4.4)$$

$$\sum \Xi_F = \dot{m}_7 (e_6^{ch} - e_7^{ch}) \quad (4.5)$$

The equations for exergy loss and exergy destruction are written on the basis of Equations (3.11) and (3.14) as follows:

$$\sum \Xi_L = \sum \Xi_F - \sum \Xi_P \quad (4.6)$$

$$\Xi_D = \sum \Xi_F - \sum \Xi_P \quad (4.7)$$

Exergy efficiency:

$$\varepsilon = (\sum \Xi_P) / (\sum \Xi_F) \quad (4.8)$$

Based on the development potential Equation (3.20), it is written as:

$$\dot{I}_{pot} = \Xi_D (1 - \varepsilon)$$

Table 4.1 Stream properties of the Reactor 401 column at the actual operation

Stream Name		**6**	**7**
Stream Phase		Vapor	Vapor
Stream Description		R1_IN	R1_OUT
Total Mass Rate	kg/s	19.41865	19.4187
Temperature	°C	500	453.2172
Pressure	kpa	3581.325	3481.325
Total Molecular Weight		22.56204	20.6578
Total Enthalpy	M*watt	37.27559	33.93723
Total Sp. Enthalpy (H)	kj/kg	1919.577	1747.658
(H0)		243.2726	266.8082
Total Sp. Entropy (S)	kj/kg°C	14.70311	14.74063
(S0)		12.61708	13.05012
Total Std. API		214.828	229.654
Bulk stream Ideal LHV	kj/m^3	50137.15	46334.71
Total Stream Ideal GHV	kj/m^3	54862.81	50671.87
Bulk stream Ideal GHV	kj/m^3	54862.81	50671.87
e(ph)	kj/kg	1054.356	1480.849
e(ch)	kj/kg	8176.906	-1526.38
Total physical Exergy	MW	20.47416	28.75617
Total CHEMICAL Exergy	MW	158.7844	-29.6404

The effect of reactor volume change on the Research Octane Number (RON) of fuels is crucial in understanding and optimizing fuel performance in engines (Table 4.2). Reactor volume directly influences the residence time of hydrocarbons within the catalytic bed, thereby impacting the extent of reactions that contribute to octane rating. A larger reactor volume typically allows for longer residence times, facilitating more complete reactions that enhance the octane rating by promoting isomerization and dehydrogenation processes. Conversely, a smaller reactor volume may reduce residence times, limiting the completion of these beneficial reactions and potentially lowering the RON.

Table 4.2 Effect change of reactor (R-401) volume of

Length (m)	Research Octane No. (C)	Aromatics (Total)
2.9	98.73	46.64
3.4	99.4	50.24
3.9	99.98	50.8
4.4	100	51.2

4.3 Exergy Analysis Calculations of the Stabilizer Column

After reaction and heating exchange steps, we need to remove light components like butane and litter from produced gasoline, so we have to make stabilization process with stabilizer column (401 E, 30 trays). This section includes the mass, energy, and exergy balances for the stabilizer column (Figure 4.2), as well as information on the relationships between exergy destruction and development potential. The stabilizer column's process is a distillation procedure. Since the distillation process converts thermal energy into chemical energy (Le Goff *et al.* 1996).

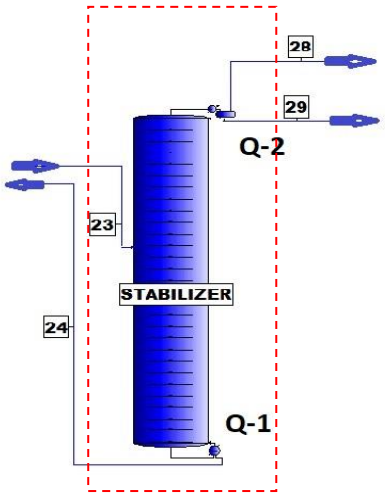

Figure 4.2 The flow chart of the stabilizer (401 E)

The equations for the stabilizer unit are given below:

Mass balance:

$$\dot{m}_{23} = \dot{m}_{24} + \dot{m}_{28} \quad (4.9)$$

Energy Balance:

$$E_{23} + E_{Q-1} = E_{24} + E_{28} + E_{Q-2} \quad (4.10)$$

Energy efficiency:

$$\eta = (E_{24} + E_{28}) / (E_{23} + E_{Q-1}) \quad (4.11)$$

The exergy equation is written based on Equation (3.13) as follows:

$$\sum \Xi_P = \dot{m}_{24} (e_{24}^{ch} - e_{23}^{ch}) + \dot{m}_{24} (e_{24}^{ph} - e_{23}^{ph}) + \dot{m}_{28} (e_{28}^{ph} - e_{23}^{ph}) \quad (4.12)$$

$$\sum \Xi_F = \Xi_{Q-1} + \dot{m}_{28} (e_{23}^{ch} - e_{28}^{ch}) \quad (4.13)$$

Equations (4.4) and (4.5) are based on to the following assumption:

$$e_{24}^{ch} < e_{23}^{ch}, \; e_{28}^{ch} < e_{23}^{ch}, \; e_{24}^{ph} > e_{23}^{ph}, \; e_{28}^{ph} > e_{23}^{ph}, \; e_{29}^{ph} > e_{23}^{ph}$$

The equations for exergy loss and exergy destruction are written based on Equations (3.11) and (3.14) as follows:

$$\sum \Xi_L = \Xi_{Q-2} + \Xi_D = \sum \Xi_F - \sum \Xi_P \quad (4.14)$$

$$\Xi_D = \sum \Xi_F - \sum \Xi_P - \Xi_{Q-2} \quad (4.15)$$

Exergy efficiency:

$$\varepsilon = (\sum \Xi_P) / (\sum \Xi_F) = \left[\sum \Xi_F - (\Xi_{Q2} + \Xi_D)\right] / (\sum \Xi_F) \quad (4.16)$$

Based on the development potential Equation (3.20), it is written as:

$$\dot{I}_{pot} = \Xi_D (1 - \varepsilon) = (\sum \Xi_F - \sum \Xi_P - \Xi_{Q2}) (1 - \varepsilon) \quad (4.17)$$

The preceding exergy equations, exergy efficiency (ε), The stabilizer column's exergy

destruction and development potential values were determined for both the intended and actual operations. For the present and proposed operations, the stabilizer column's stream characteristics are provided in Tables 4.3 and 4.4, respectively.

Table 4.3 Streams characteristics of the stabilizer column at actual operation

Stream Name(phase)		**23(Liq-Vap)**	**24(liq)**	**28(vap)**	**29(vap)**
Stream Phase		Mixed	Liquid	Vapor	Liquid
Stream Description		BOTTOM		LPG	
Total Mass Rate	**kg/s**	9.98	9.01	0.31	0.67
Temperature	**°C**	130.00	248.89	31.96	31.96
Pressure	**kPa**	2831.33	2471.33	2331.33	2331.33
Total Molecular Weight		84.76	97.80	31.26	42.13
Total Enthalpy	**MW**	2.86	5.41	0.11	0.06
Spesific Enthalpy (h)	**kJ/kg**	286.86	600.13	375.43	89.91
Spesific Enthalpy (h_0)	**kJ/kg**	99.28	54.94	410.39	424.05
Spesific Entropy (s)	**kJ/kg.°C**	6.52	7.01	8.79	6.85
Spesific Entropy (s_0)	**kJ/kg.°C**	6.04	5.69	9.69	8.44
Bulk stream Ideal LHV	**kJ/m^3**	169399.70	194528.10	66244.43	87287.82
Total Stream Ideal GHV	**kJ/m^3**	180250.50	206435.10	72357.23	94935.91
$e^{(ph)}$	**kJ/kg**	45.03	151.24	232.97	138.47
$e^{(ch)}$	**kJ/kg**	47147.28	46683.49	11858.55	33087.84
Total Physical Exergy	**MW**	0.45	1.36	0.071	0.092
Total Chemical Exergy	**MW**	470.67	420.51	3.63	22.14

Table 4.4 Streams characteristics of the stabilizer column at proposed operation

Stream Name(phase)		**23(Liq-Vap)**	**24(liq)**	**28(vap)**	**29(vap)**
Stream Phase		Mixed	Liquid	Vapor	Liquid
Stream Description		BOTTOM		LPG	
Total Mass Rate	**kg/s**	9.98	9.01	0.31	0.67
Temperature	**°C**	130.00	248.89	31.96	31.96
Pressure	**kPa**	2831.33	2471.33	2331.33	2331.33
Total Molecular Weight		84.76	97.80	31.26	42.13
Total Enthalpy	**MW**	2.86	5.41	0.11	0.06
Spesific Enthalpy (h)	**kJ/kg**	286.86	600.13	375.43	89.91
Spesific Enthalpy (h_0)	**kJ/kg**	99.28	54.94	410.39	424.05
Spesific Entropy (s)	**kJ/kg.°C**	6.52	7.01	8.79	6.85
Spesific Entropy (s_0)	**kJ/kg.°C**	6.04	5.69	9.69	8.44
Bulk stream Ideal LHV	**kJ/m^3**	169399.70	194528.10	66244.43	87287.82

Table 4.4 Streams characteristics of the stabilizer column at proposed operation (Continued)

Total Stream Ideal GHV	**kJ/m^3**	180250.50	206435.10	72357.23	94935.91
$e^{(ph)}$	**kJ/kg**	45.03	545.19	-34.95	-334.14
$e^{(ch)}$	**kJ/kg**	47147.28	46683.49	11858.55	33087.84
Total Physical Exergy	**MW**	0.45	4.91	0.071	0.092
Total Chemical Exergy	**MW**	470.67	420.51	3.63	22.14

The suggested operation's energy efficiency has enhanced, as shown by Table 4.5 findings. The suggested operation's exergy consumption and development potential are both reduced.

Table 4.5 The results of the exergy analysis of stabilizer at actual and proposed operation

		Act. Operation	**Prop. Operation**
Ξ_P	**(MW)**	49.41	48.15
Ξ_F	**(MW)**	52.05	51.31
Ξ_D	**(MW)**	5.23	4.95
η	**(%)**	43.40	48.30
ε	**(%)**	94.35	93.84
$\dot{I}_{pot}$	**(MW)**	2.15	1.87
E_{Q-1}	**(MW)**	10	8.7
E_{Q-2}	**(MW)**	4.5	3.27
Ξ_{Q-1}	**(MW)**	8.90	7.70
Ξ_{Q-2}	**(MW)**	2.91	1.83

Table 4.6 Process variables result in reforming process

Variables	**Value**	**units**
Reformate RON	99.66811	-
Sum of Aromatics	49.42765	wt. %
LHSV	0.662965	-
C5+ MON	77.23843	-
Calibration H_2/HC Ratio - mol/mol	1.6	-

4.4 Reformer H_2/HC Ratio effect on RON

H_2/HC Ratio is one of the important parameters which has a big effect on RON yield so we studied the H_2/HC Ratio on range (0.5-2.6) by step value 0.3 on Reformate RON, Sum of Aromatics and LHSV, and the result is shown in Table 4.7.

Table 4.7 Effect of H_2/HC on reformate yields

H_2/HC ratio	Reformate Octane Number	LHSV	Sum of aromatic
0.5	98.31	0.663	49.97
0.8	98.76	0.663	49.85
1.1	99.16	0.663	49.71

We can observe that when the ratio increases the RON increase till it reached the biggest value 99.1 and this result is the same result in literature review chapter.

4.5 Calculations of the Heating Furnace (F-401)

Utilizing this furnace, the feed stream from the HX-401 is heated to a maximum of 296.5 ^oC. The reference environment model was the calculation of the chemical exergy of the air. The e^{ch} of the fuel was calculated on the basis of Equation (3.8) using the data obtained from the simulation study (Ancheyta-Juarez *et al.* 2001).

The flow chart of the heating furnace F-401 is shown in Figure 4.3, and the air composition values used in the calculations are given in Table 4.8.

Table 4.8 Composition of air (Gaggioli 1983)

Component	**N_2**	**O_2**	**CO_2**	**$H_2O(g)$**
Composition (v/v, %)	77,48	20,59	0,03	1,90
e^{ch} (kJ/kg)	26	124	451	527

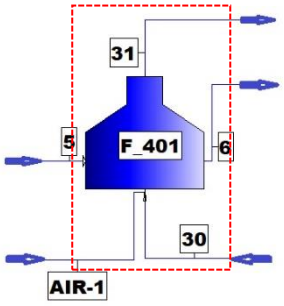

Figure 4.3 Flow chart of the heating furnace (F-401)

The following equations represent the energy and exergy balances, efficiencies, exergy destruction, and development potentials for the heating furnace F-401 under both the proposed and actual operating conditions.

The equations for the Furnace are given below:

Energy Balance:

$$E_5 + E_{30} = E_6 + E_{31} \tag{4.18}$$

Energy efficiency:

$$\eta = E_6 / (E_{30} + E_5) \tag{4.19}$$

The exergy equation is written on the basis of Equation (3.13) as follows:

$$\sum \Xi_P = (\Xi_6^{ph} - \Xi_5^{ph} + \Xi_{air}^{ph}) \tag{4.20}$$

$$\sum \Xi_F = \Xi_{30}^{ch} + \Xi_{air}^{ch} \tag{4.21}$$

$\dot{\Xi}_L$ and $\dot{\Xi}_D$ are written on the basis of the Equations (3.11) and (3.14). Here, the exergy thrown out with the flue gases is also included in the exergy destruction and the calculation is made:

$$\sum \Xi_D = \sum \Xi_F - \sum \Xi_P = (\Xi_{30}^{ch} + \Xi_{air}^{ph}) - (\Xi_6^{ph} - \Xi_5^{ph} - \Xi_{air}^{ph}) \tag{4.22}$$

Exergy efficiency (ε):

$$\varepsilon = (\sum \Xi_P) / (\sum \Xi_F) = (\Xi_6^{ph} - \Xi_5^{ph} - \Xi_{air}^{ph}) / (\Xi_{30}^{ch} + \Xi_{air}^{ph}) \quad (4.23)$$

It is expressed as follows using the development potential Equation (3.20):

$$\dot{I}_{pot} = \sum \Xi_D (1- \varepsilon) = (\Xi_6^{ph} - \Xi_5^{ph} - \Xi_{air}^{ph}) * (1- \varepsilon) \quad (4.24)$$

By using the exergy equations above, exergy efficiency (ε) and development potential values for the for heating furnace F-401 were calculated.

Tables 4.9 and 4.10, respectively, present the heating furnace F-401's stream characteristics under the proposed and actual operating conditions. Table 4.11 shows the outcomes of the exergy analysis for the actual and proposed operations

Table 4.9 Streams characteristics of the heating furnace F-401 at actual operation

Stream Name		**5**	**6**	**30**	**31**
Stream Phase		Vapor	Vapor	Vapor	Vapor
Stream Description			R1_IN	FUEL 1	
Total Mass Rate	**kg/s**	19.42	19.42	45.10	770.69
Temperature	**ºC**	375.00	500.00	25.00	1922.23
Pressure	**kPa**	3581.33	3581.33	901.33	901.33
Total Molecular Weight		22.56	22.56	30.07	28.23
Total Enthalpy	**MW**	27.97	37.28	15.78	2162.16
Spesific Enthalpy (h)	**kJ/kg**	1440.19	1919.58	349.95	2805.47
Spesific Enthalpy (h_0)	**kJ/kg**	243.27	243.27	364.79	97.89
Spesific Entropy (s)	**kJ/kg.ºC**	14.03	14.70	9.21	9.07
Spesific Entropy (s_0)	**kJ/kg.ºC**	12.62	12.62	9.84	6.19
Bulk stream Ideal LHV	**kJ/m^3**	50137.15	50137.15	63399.28	n/a
Total Stream Ideal GHV	**kJ/m^3**	54862.81	54862.81	69343.04	n/a
$e^{(ph)}$	**kJ/kg**	776.36	1676.30	-14.85	2707.58
$e^{(ch)}$	**kJ/kg**	8176.91	8176.91	9966.70	45813.52
Total Physical Exergy	**MW**	15.08	32.55	-0.67	2086.71
Total Chemical Exergy	**MW**	158.78	158.78	449.54	35308.24

Table 4.10 Streams characteristics of the heating furnace F-401 at proposed operation

Stream Name		**5**	**6**	**30**	**31**
Stream Phase		Vapor	Vapor	Vapor	Vapor
Stream Description			R1_IN	FUEL 1	
Total Mass Rate	**kg/s**	19.42	19.42	45.10	770.69
Temperature	**°C**	375.00	500.00	25.00	1922.23
Pressure	**kPa**	3581.33	3581.33	901.33	901.33
Total Molecular Weight		22.56	22.56	30.07	28.23
Total Enthalpy	**MW**	27.97	37.28	15.78	2162.16
Spesific Enthalpy (h)	**kJ/kg**	1440.19	1919.58	349.95	2805.47
Spesific Enthalpy (h_0)	**kJ/kg**	243.27	243.27	364.79	97.89
Spesific Entropy (s)	**kJ/kg.°C**	14.03	14.70	9.21	9.07
Spesific Entropy (s_0)	**kJ/kg.°C**	12.62	12.62	9.84	6.19
Bulk stream Ideal LHV	**kJ/m^3**	50137.15	50137.15	63399.28	n/a
Total Stream Ideal GHV	**kJ/m^3**	54862.81	54862.81	69343.04	n/a
$e^{(ph)}$	**kJ/kg**	776.36	1676.30	-14.85	2707.58
$e^{(ch)}$	**kJ/kg**	8176.91	8176.91	9966.70	45813.52
Total Physical Exergy	**MW**	15.08	32.55	-0.67	2086.71
Total Chemical Exergy	**MW**	158.78	158.78	449.54	35308.24

Table 4.11 The results of the exergy analysis at actual and proposed operation of F-401

		Actual	**Proposed**
Ξ_P	**(MW)**	17.47	15.36
Ξ_F	**(MW)**	10.7	9.21
Ξ_D	**(MW)**	2.34	3.35
η	**(%)**	85	87
ε	**(%)**	78	79
I_{pot}	**(MW)**	5.27	5.01

The heating furnaces F-401 were found to have energy efficiency of 85% and 87% under actual and proposed operation, respectively. The computed exergy efficiencies were 78% and 79%, respectively. The corresponding exergy destructions were 2.34 MW and 3.35 MW, while the corresponding development potentials were 5.27 MW and 5.01 MW.

4.6 Calculations of Heat Exchangers

The streams are heated or cooled using the heat exchanger network. The Reformer unit consists of five heat exchangers (HX-401, HX-402, HX-403, HX-404, and HX-405) in total.

4.6.1 Heat Exchanger (HX-401)

The equations created as a result of the heat exchanger study are provided here for the heat exchangers HX-401, HX-402, HX-403, HX-404, and HX-405. The HX-1 flowchart. The outlet stream of the heating furnace F-401 heats the Feedstock and Recycled Gas mixture for the HX-401.

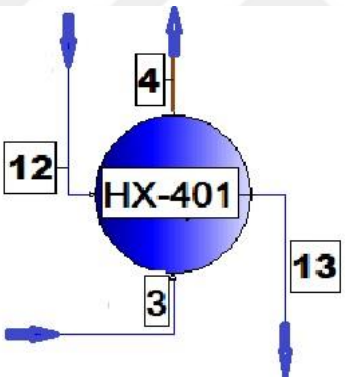

Figure 4.4 Flow chart of the HX-401

The HX-401 heat exchanger's (Figure 4.4) mass, energy, and exergy balances, as well as its exergy destruction and development potential formulae, are provided below for both real and hypothetical operation.

Mass balance:

$$\dot{m}_3 = \dot{m}_4 \tag{4.25}$$

$$\dot{m}_{13} = \dot{m}_{12} \tag{4.26}$$

Energy Balance:

$$E_3 + E_{12} = E_4 + E_{13} \quad (4.27)$$

Energy efficiency:

$$\eta = (E_4 - E_3) / (E_{12} - E_{13}) \quad (4.28)$$

$$\sum \Xi_P = \Xi_4 - \Xi_3 \quad (4.29)$$

$$\sum \Xi_F = \Xi_{12} - \Xi_{13}$$

$$\Xi_D = \sum \Xi_F - \sum \Xi_P \quad (4.30)$$

Exergy efficiency:

$$\varepsilon = (\sum \Xi_P) / (\sum \Xi_F) = (\Xi_4 - \Xi_3) / (\Xi_{12} - \Xi_{13}) \quad (4.31)$$

On the basis of the development potential Equation (3.20), it is written as:

$$\dot{I}_{pot} = \Xi_D (1- \varepsilon) = (\sum \Xi_F - \sum \Xi_P)(1- \varepsilon) \quad (4.32)$$

Tables 4.12 and 4.13, which describe the HX-401's stream characteristics under actual and proposed operation, respectively. Table 4.14 contains the findings of the exergy analysis at the proposed and actual operation.

The HX-401 energy efficiency at both proposed and actual operation were found to be 99.9%. The computed exergy efficiencies were 78% and 79%, respectively. Development potentials were calculated to be 8.5 MW and 8.44 MW, respectively, while exergy destructions were 2.96 MW and 2.64 MW, respectively.

Table 4.12 Stream characteristics of heat exchanger HX-401 at actual operation

Stream Name		**3**	**4**	**12**	**13**
Stream Phase		Mixed	Vapor	Vapor	Vapor
Stream Description					
Total Mass Rate	kg/s	19.42	19.42	19.42	19.42
Temperature	°C	76.19	210.00	343.21	176.80
Pressure	kPa	3621.32	3601.32	3261.32	3241.32
Total Molecular Weight		22.56	22.56	19.53	19.53
Total Enthalpy	MW	6.20	16.98	26.04	15.26
Spesific Enthalpy (h)	kJ/kg	319.03	874.20	1341.18	786.01
Spesific Enthalpy (h_0)		243.27	243.27	286.61	286.61
Spesific Entropy (s)	kJ/kg.°C	12.62	12.62	13.29	13.29
Spesific Entropy (s_0)		13.02	14.26	13.22	13.29
Bulk stream Ideal LHV	kJ/m^3	50137.20	50137.20	44076.50	44076.50
Total Stream Ideal GHV	kJ/m^3	54862.80	54862.80	48189.50	48189.50
$\mathbf{e^{(ph)}}$	kJ/kg	196.27	630.93	1054.58	499.41
$\mathbf{e^{(ch)}}$	kJ/kg	8176.93	8176.93	-9907.63	-9907.63
Total Physical Exergy	MW	3.81	12.25	20.48	9.70
Total Chemical Exergy	MW	158.78	158.78	-192.39	-192.39

Table 4.13 Stream characteristics of heat exchanger HX-401 at proposed operation

Stream Name		**3**	**4**	**12**	**13**
Stream Phase		Mixed	Vapor	Vapor	Vapor
Stream Description					
Total Mass Rate	kg/s	19.42	19.42	19.42	19.42
Temperature	°C	76.19	210.00	343.21	176.80
Pressure	kPa	3621.32	3601.32	3261.32	3241.32
Total Molecular Weight		22.56	22.56	19.53	19.53
Total Enthalpy	MW	6.20	16.98	26.04	15.26
Spesific Enthalpy (h)	kJ/kg	319.03	874.20	1341.18	786.01
Spesific Enthalpy (h_0)		243.27	243.27	286.61	286.61
Spesific Entropy (s)	kJ/kg.°C	12.62	12.62	13.29	13.29
Spesific Entropy (s_0)		13.02	14.26	13.22	13.29
Bulk stream Ideal LHV	kJ/m^3	50137.20	50137.20	44076.50	44076.50
Total Stream Ideal GHV	kJ/m^3	54862.80	54862.80	48189.50	48189.50
$\mathbf{e^{(ph)}}$	kJ/kg	196.27	630.93	1054.58	499.41
$\mathbf{e^{(ch)}}$	kJ/kg	8176.93	8176.93	-9907.63	-9907.63
Total Physical Exergy	MW	3.81	12.25	20.48	9.70
Total Chemical Exergy	MW	158.78	158.78	-192.39	-192.39

Table 4.14 The exergy analysis results at actual and proposed operation of HX-401

		Actual	Proposed
Ξ_P	(MW)	8.5	8.44
Ξ_F	(MW)	10.78	10.05
Ξ_D	(MW)	2.96	2.64
η	(%)	78.3	78.9
ε	(%)	78	79
$\dot{I}_{pot}$	(MW)	0.51	0.56

4.6.2 Heat Exchanger (HX-402)

The exit stream (Stram4) of the HX-401 which is used in the heat exchanger HX-402, heats the (Stream 5). Figure 4.5 displays the HX-402 flowchart.

The mass, energy, and exergy balances, as well as the exergy and energy efficiencies, exergy destruction, and development potential for actual and projected operation (Figure 4.6), are calculated here for the analysis of the heat exchanger HX-402 (Lai *et al*. 2018). Tables 4.15 and 4.16, which describe the HX-402 stream characteristics under real and proposed operation, respectively. Table 4.17 contains the findings of the exergy study for the actual and proposed operations.

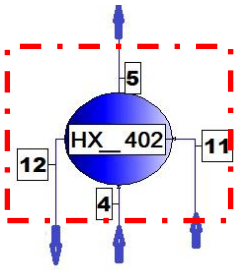

Figure 4.5 Flow chart of the HX-402

Table 4.15 Stream characteristics of heat exchanger HX-402 at actual operation

Stream Name		4	5	11	12
Stream Phase		Vapor	Vapor	Vapor	Vapor
Stream Description				R403_OUT	
Total Mass Rate	kg/s	19.42	19.42	19.42	19.42
Temperature	°C	210.00	375.00	493.17	343.21
Pressure	kPa	3601.33	3581.33	3281.33	3261.33
Total Molecular Weight		22.56	22.56	19.53	19.53
Total Enthalpy	MW	16.98	27.97	37.03	26.04
Spesific Enthalpy (h)	kJ/kg	874.20	1440.19	1907.17	1341.18
Spesific Enthalpy (h_0)		243.27	243.27	286.61	286.61
Spesific Entropy (s)	kJ/kg.°C	13.02	14.03	15.08	14.26
Spesific Entropy (s_0)		12.62	12.62	13.29	13.29
Bulk stream Ideal LHV	kJ/m^3	50137.15	50137.15	44076.54	44076.54
Total Stream Ideal GHV	kJ/m^3	54862.81	54862.81	48189.54	48189.54
$e^{(ph)}$	kJ/kg	510.40	1196.91	1620.56	1054.58
$e^{(ch)}$	kJ/kg	8176.91	8176.91	-9907.56	-9907.56
Total Physical Exergy	MW	9.91	23.24	31.47	20.48
Total Chemical Exergy	MW	158.78	158.78	-192.39	-192.39

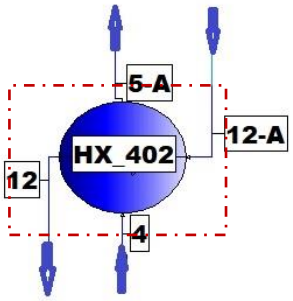

Figure 4.6 Flow chart of the HX-402 after proposed operation

Table 4.16 Stream characteristics of heat exchanger HX-402 at proposed operation

Stream Name		4	5-A	12-A	12
Stream Phase		Vapor	Vapor	Vapor	Vapor
Stream Description					
Total Mass Rate	kg/s	19.42	19.42	19.42	19.42
Temperature	°C	210.00	300.00	399.62	343.21
Pressure	kPa	3601.33	3581.33	3281.33	3261.33

Table 4.16 Stream characteristics of heat exchanger HX-402 at proposed operation (Continued)

Total Molecular Weight		22.56	22.56	19.53	19.53
Total Enthalpy	MW	16.98	22.78	30.05	26.04
Spesific Enthalpy (h)	kJ/kg	874.20	1172.89	1547.27	1341.18
Spesific Enthalpy (h_0)		243.27	243.27	286.61	286.61
Spesific Entropy (s)	kJ/kg.^oC	13.02	13.59	14.58	14.26
Spesific Entropy (s_0)		12.62	12.62	13.29	13.29
Bulk stream Ideal LHV	kJ/m^3	50137.15	50137.15	44076.54	44076.54
Total Stream Ideal GHV	kJ/m^3	54862.81	54862.81	48189.54	48189.54
$\mathbf{e^{(ph)}}$	kJ/kg	510.40	929.62	1260.66	1054.58
$\mathbf{e^{(ch)}}$	kJ/kg	8176.91	8176.91	-9907.57	-9907.56
Total Physical Exergy	MW	9.91	18.05	24.48	20.48
Total Chemical Exergy	MW	158.78	158.78	-192.39	-192.39

Table 4.17 Exergy analysis resultss related to heat exchanger HX-402 at actual and proposed operation

		Act. Operation	**Prop. Operation**
Ξ_P	**(MW)**	13.33	8.14
Ξ_F	**(MW)**	10.99	9.09
Ξ_D	**(MW)**	2.34	4.14
η	**(%)**	99.9	99.9
ε	**(%)**	99.9	99.9
$\dot{I}_{pot}$	**(MW)**	0.49	0.38

The HX-402 was shown to have energy efficiency of 99.9% for both actual and proposed operation. The computed exergy efficiencies were 99% and 99%, respectively. Exergy destructions were estimated to be 2.314 MW and 0.06 MW, whereas development proposed were estimated to be 0.498 MW and 0.501 MW, respectivey.

4.6.3 Heat Exchanger (HX-403)

In this heat exchanger (Stream 5-A) heats the (Stream 11) for the heat exchanger HX-403. Figure 4.7 displays the flowchart for the HX-403.

In this analysis of the heat exchanger HX-403, the equations from 4.17 to 4.24 are utilized to determine the mass, energy, and exergy balances as well as the energy and exergy efficiencies, exergy destruction, and development potential for present and proposed operation.

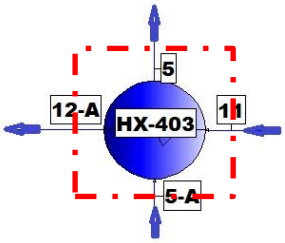

Figure 4.7 Flow chart of the HX-403

Tables 4.18 and 4.19, respectively, provide information on the stream characteristics of the HX-403 during actual and proposed operation. Table 4.20 contains the findings of the exergy study for the actual and proposed operations.

Table 4.18 Stream characteristics of heat exchanger HX-403 at actual operation

Stream Name		**5-A**	**5**	**11**	**12-A**
Stream Phase		**Vapor**	**Vapor**	**Vapor**	**Vapor**
Stream Description				**R-403OUT**	
Total Mass Rate	kg/s	19.42	19.42	19.42	19.42
Temperature	°C	300.00	375.00	493.17	399.62
Pressure	kPa	3581.33	3581.33	3281.33	3281.33
Total Molecular Weight		22.56	22.56	19.53	19.53
Total Enthalpy	MW	22.78	27.97	37.03	30.05
Spesific Enthalpy (h)	kJ/kg	1172.89	1440.19	1907.17	1547.27
Spesific Enthalpy (h_0)		243.27	243.27	286.61	286.61
Spesific Entropy (s)	kJ/kg.°C	13.59	14.03	15.08	14.58
Spesific Entropy (s_0)		12.62	12.62	13.29	13.29
Bulk stream Ideal LHV	kJ/m^3	50137.15	50137.15	44076.54	44076.54
Total Stream Ideal GHV	kJ/m^3	54862.81	54862.81	48189.54	48189.54
$\mathbf{e^{(ph)}}$	kJ/kg	929.62	1196.91	1620.56	1260.66
$\mathbf{e^{(ch)}}$	kJ/kg	8176.91	8176.91	-9907.56	-9907.57
Total Physical Exergy	MW	18.05	23.24	31.47	24.48
Total Chemical Exergy	MW	158.78	158.78	-192.39	-192.39

Table 4.19 Stream characteristics of heat exchanger HX-403 at proposed operation

Stream Name		**5-A**	**5**	**11**	**12-A**
Stream Phase		**Vapor**	**Vapor**	**Vapor**	**Vapor**
Stream Description				**R-403OUT**	
Total Mass Rate	kg/s	19.42	19.42	19.42	19.42
Temperature	°C	300.00	375.00	493.17	399.62
Pressure	kPa	3581.33	3581.33	3281.33	3281.33
Total Molecular Weight		22.56	22.56	19.53	19.53
Total Enthalpy	MW	22.78	27.97	37.03	30.05
Spesific Enthalpy (h)	kJ/kg	1172.89	1440.19	1907.17	1547.27
Spesific Enthalpy (h_0)		243.27	243.27	286.61	286.61
Spesific Entropy (s)	kJ/kg.°C	13.59	14.03	15.08	14.58
Spesific Entropy (s_0)		12.62	12.62	13.29	13.29
Bulk stream Ideal LHV	kJ/m^3	50137.15	50137.15	44076.54	44076.54
Total Stream Ideal GHV	kJ/m^3	54862.81	54862.81	48189.54	48189.54
$\mathbf{e^{(ph)}}$	kJ/kg	929.62	1196.91	1620.56	1260.66
$\mathbf{e^{(ch)}}$	kJ/kg	8176.91	8176.91	-9907.56	-9907.57
Total Physical Exergy	MW	18.05	23.24	31.47	24.48
Total Chemical Exergy	MW	158.78	158.78	-192.39	-192.39

Table 4.20 Exergy analysis resultss related to heat exchanger HX-403 at actual and proposed operation

		Act. Operation	**Prop. Operation**
Ξ_P	**(MW)**	5.19	4.98
Ξ_F	**(MW)**	6.98	6.98
Ξ_D	**(MW)**	1.34	1.34
η	**(%)**	74.3	74.3
ε	**(%)**	74.3	74.3
$\dot{I}_{pot}$	**(MW)**	0.34	0.34

The HX-403 was shown to have energy efficiency of 74.3% for both actual and proposed operation. The computed exergy efficiencies were 74% and 74%, respectively. The corresponding exergy destructions were 1.346 MW and 1.346 MW, while the corresponding development potentials were 0.346 MW and 0.346 MW.

4.6.4 Compressor (402J)

Calculations are made regarding the mass, energy, and exergy balances, as well as the exergy destruction and development potential for both the proposed and actual operations.

The Compressor (402J)'s (Figure 4.8) stream characteristics at both the proposed and actual operating conditions are shown in Table 4.21. The Table 4.22 contains the findings of the exergy study for the actual and proposed operations.

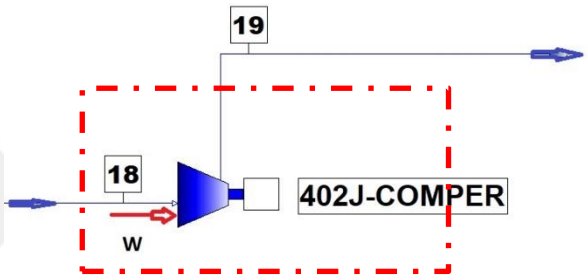

Figure 4.8 Flow chart of the Compressor 402J

The following equations represent the mass, energy, and exergy balances, as well as the exergy destruction and development potential equations for the HX-404.

Mass balance:

$$\dot{m}_{18} = \dot{m}_{19} \quad (4.33)$$

Energy Balance:

$$E_w = E_{19} - E_{18} \quad (4.34)$$

Energy efficiency:

$$\eta = (E_{19} - E_{18}) / (E_w) \quad (4.35)$$

$$\sum \Xi_p = \Xi_{19} - \Xi_{18} \quad (4.36)$$

$$\sum \Xi_F = \Xi_w \quad (4.37)$$

$$\Xi_D = \sum \Xi_F - \sum \Xi_P \quad (4.38)$$

Exergy efficiency:

$$\varepsilon = (\sum \Xi_P / \sum \Xi_F) \quad (4.39)$$

On the basis of the development potential Equation (3.20), it is written as:

$$\dot{I}_{pot} = \Xi_D (1- \varepsilon) \quad (4.40)$$

The energy efficiencies of the Comp-402J at actual and proposed operation were found to be 100% and 100 %, respectively. Exergy efficiencies were calculated as 39 % and 39 %, respectively. Exergy destructions were 0.75 MW and 0.75003MW, respectively; development potentials were determined as 3.726 MW and 3.726 MW, respectively.

Table 4.21 Stream characteristics of Comp-402J at actual and proposed operation

Stream Name		**18.00**	**19.00**
Stream Phase		**Vapor**	**Vapor**
Stream Description			
Total Mass Rate	kg/s	1.10	1.10
Temperature	°C	43.00	82.88
Pressure	kPa	2401.33	4101.33
Total Molecular Weight		10.76	10.76
Total Enthalpy	MW	0.44	0.60
Spesific Enthalpy (h)	kJ/kg	403.31	540.26
Spesific Enthalpy (h_0)		357.12	357.12
Spesific Entropy (s)	kJ/kg.°C	18.18	18.18
Spesific Entropy (s_0)		20.46	20.46
Bulk stream Ideal LHV	kJ/m^3	27242.29	27242.29
Total Stream Ideal GHV	kJ/m^3	30450.22	30450.22
$e^{(ph)}$	kJ/kg	726.53	183.13
$e^{(ch)}$	kJ/kg	-284485.00	-284485.00
Total Physical Exergy	MW	0.80	0.20
Total Chemical Exergy	MW	-313.62	-313.62

Table 4.22 Exergy analysis results related to Comp-402J actual and proposed operation

		Act. Operation	Prop. Operation
Ξ_P	(MW)	0.59	0.57
Ξ_F	(MW)	0.15	0.15
Ξ_D	(MW)	0.45	0.75
η	(%)	100	100
ε	(%)	99	99
$\dot{I}_{pot}$	(MW)	1.32	1.45

4.7 Comparison of Exergy Analysis Results

The results of the exergy analysis performed in this study at actual and proposed operation are given below in a graphical and comparative manner. The exergy efficiencies obtained for each process equipment are shown in Figure 4.9.

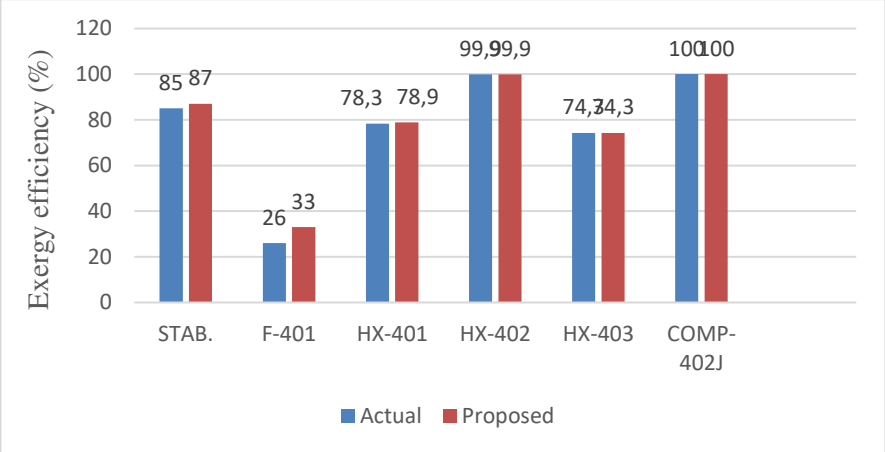

Figure 4.9 Exergy efficiencies of process equipment

When the energy efficiencies of the process equipment were examined, the stabilizer's 83% exergy effeciency at proposed and actual operation is 86% was found to be the greatest.

At actual and proposed operation, the furnace's lowest exergy efficiency was found to be 85% and 87%, respectively.

And the main reason for increasing the efficiency of the furnace is the addition of a third heat exchange HX-403, the exergy efficiency of the heat exchanger HX-403 is bigger than that of the other heat exchangers. Figure 4.10 displays the process equipment's exergy destruction values. The analysis of 4.10 reveals that.

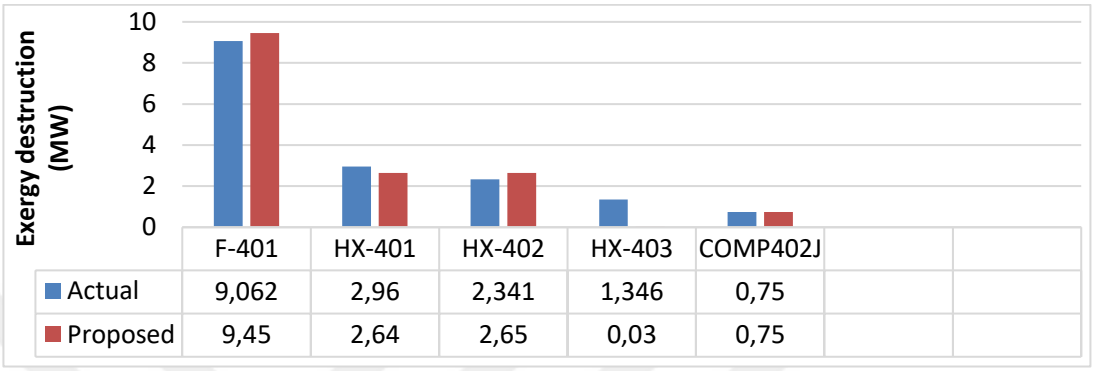

Figure 4.10 Exergy destruction values of process components

The maximum improvement that can be done by reducing the exergy loss, that is, the development potential values are shown in Figure 4.11.

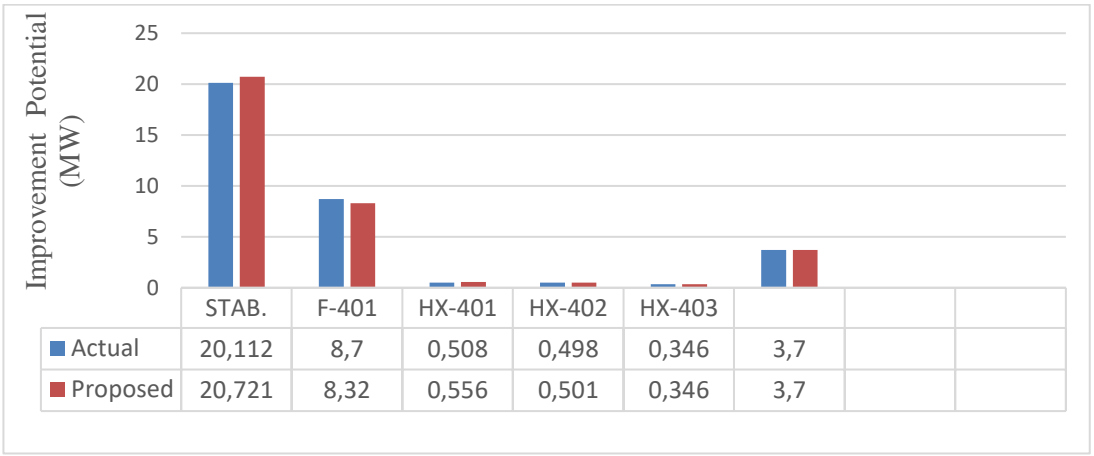

Figure 4.11 Comparison of process components development potentials at actual and proposed operation

The F-401 region has the highest values for development potential (6.45 MW) for proposed operation and (9.062) MW for actual operation.

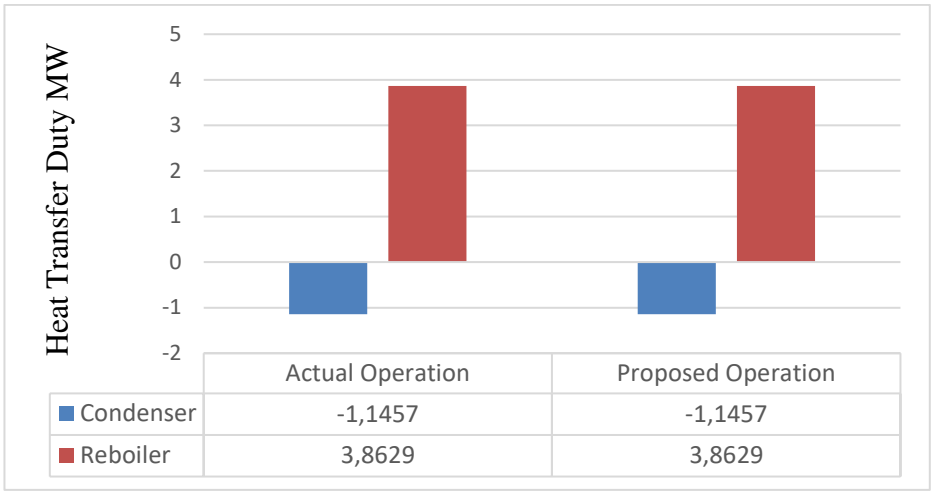

Figure 4.12 The comparison of reboiler and condenser duties of Stabilizer for actual and proposed operation

The comparison of the temperature of Stabilizer trays for actual and proposed operation are shown in Figure 4.13.

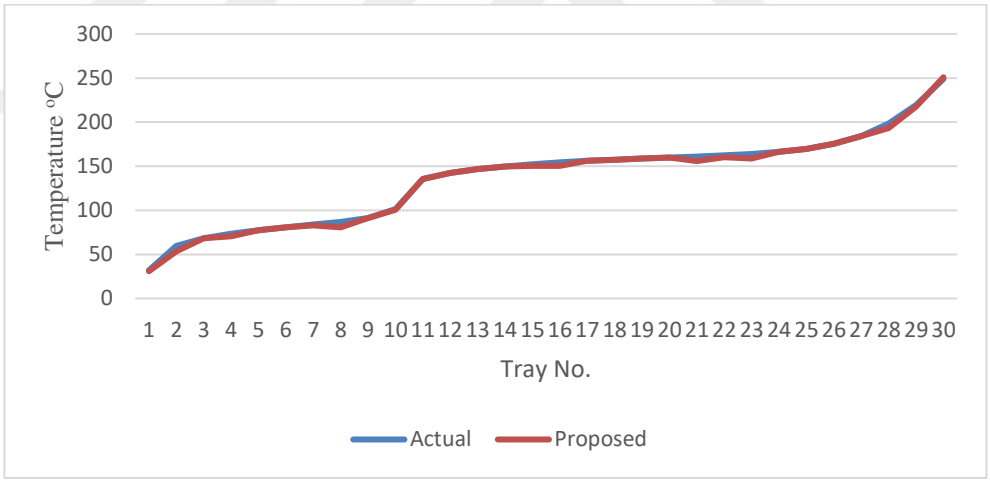

Figure 4.13 Shows the temperature of Stabilizer trays for the proposed and actual operations

The trays' stabilizer temperature comparison reveals that they were quite near for both the proposed and actual operations.

4.8 Material Balance for the Overall Process at Actual and Proposed Operation

The total material balance for the actual and proposed operations of the Reformer Unit are shown in Tables 4.23 and 4.24, respectively, in accordance with the overall process of the Reformer unit as shown in the block diagrams Figures 4.14 and Figures 4.15 for the actual and proposed operations, respectively.

Table 4.23 Mass flow rate of inlet streams to the Reformer unit at actual and proposed operating conditions

Inlet	**Actual Operating**	**Proposed Operating**
	kg/s	kg/s
Feedstock (HN Feed)	11.08531	
Hydrogen Gas	8.33	8.000
Total Inlet	19.41865	19.3850

Table 4.24 Mass flow rate of outlet streams from the Reformer unit at actual and proposed operating conditions

Outlet	**Act. Operating**	**Prop. Operating**
	kg/s	kg/s
Reformer Product	9.982958	9.008
Out Gas to Gas Oil Reformer unit	0.306128	0.3060
HC-Gas to LPG unit	0.669083	0.66923
Total Outlet	10.958169	9.98323

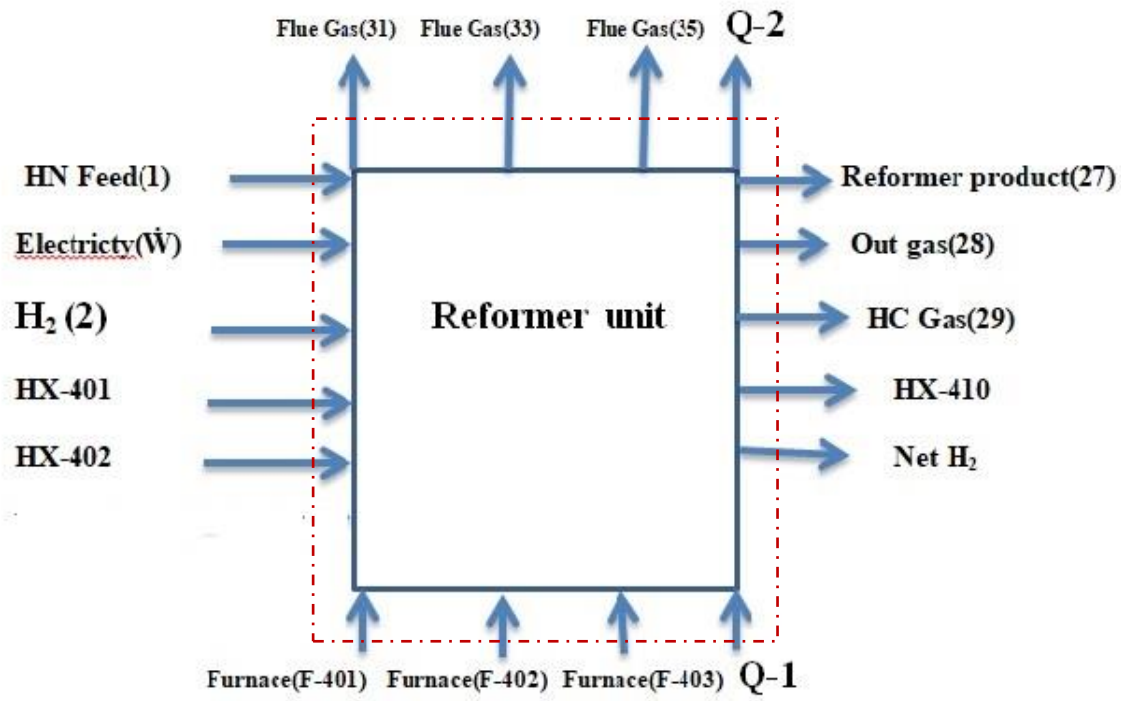

Figure 4.14 The block diagram of total energy balance for the actual operation of the Reformer Unit

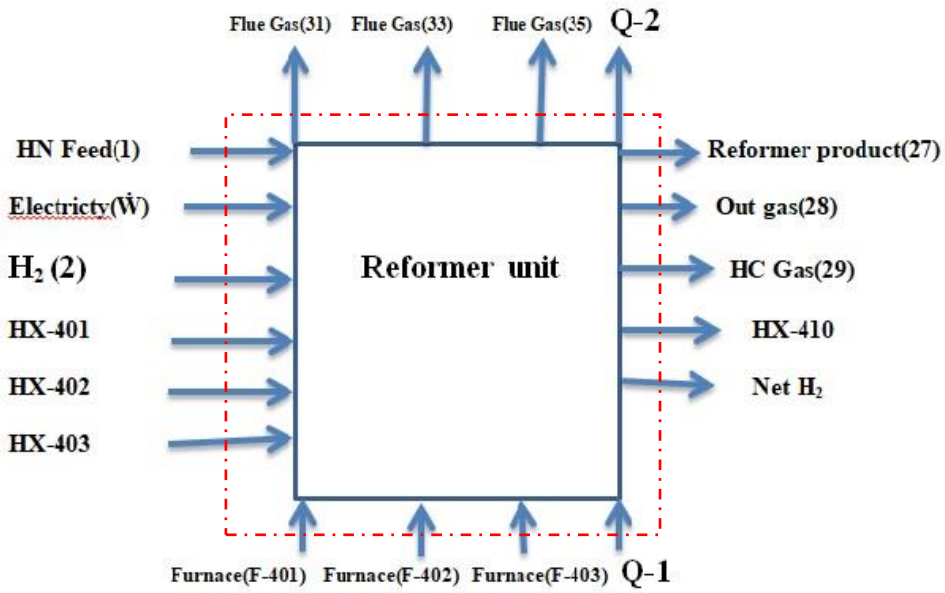

Figure 4.15 The block diagram of the total energy balance of the Reformer unit at the proposed operation

4.9 Energy Balance of the Overall Process at Actual and Proposed Operation

According to the flow charts, the total energy balance and energy efficiency for the actual and proposed operation of the Reformer Unit are illustrated below (Figures 4.14 and 4.15, respectively).

Total Energy Balance of the unit for actual operation:

$$E_1 + \dot{W} + E_2 + E_{F\text{-}1} + E_{F40\text{-}2} + E_{F\text{-}403} + E_{Q\text{-}1} + E_{HX\text{-}401} + E_{HX\text{-}402} = E_{27} + E_{Q\text{-}2} + E_{28} + E_{29} + E_{31} + E_{33} + E_{35} + E_{HX\text{-}410} + E_{H2(17)} \quad (4.41)$$

Energy efficiency:

$$\eta = E_{27} / E_1 + \dot{W} + E_2 + E_{F\text{-}401} + E_{F\text{-}402} + E_{F\text{-}403} + E_{Q\text{-}1} + E_{HX\text{-}401} + E_{HX\text{-}402} + E_{H2(17)} \quad (4.42)$$

Total Energy Balance of the unit for proposed operation:

$$E_1 + \dot{W} + E_2 + E_{F\text{-}401} + E_{F\text{-}402} + E_{F\text{-}403} + E_{Q\text{-}1} + E_{HX\text{-}403} = E_{27} + E_{R\text{-}402} + E_{28} + E_{29} + E_{33} + E_{HX\text{-}404} + E_{HX\text{-}405} + E_{34} + E_{H2(17)} \quad (4.43)$$

Energy efficiency:

$$\eta = E_{27} / E_1 + \dot{W} + E_2 + E_{F\text{-}401} + E_{F\text{-}402} + E_{F\text{-}403} + E_{R\text{-}401} + E_{HX\text{-}401} + E_{HX\text{-}402} + E_{HX\text{-}403} \quad (4.53)$$

4.10 Exergy Balance of the Overall Process at Actual and Proposed Operation

As demonstrated in the block diagrams (Figures 4.14 and 4.15, respectively), the total process's exergy efficiencies, exergy destruction, and development potential equations are provided below.

The exergy equations for the actual and proposed operation are written on the basis of Equation (3.13) as follows:

$$\sum \Xi_P = \Xi_{27} + \Xi_{28} + \Xi_{29} - \Xi_1 - \Xi_2 \quad \text{(actual and proposed operation)} \quad (4.44)$$

$$\sum \Xi_F = \Xi_w + \Xi_{27} + \Xi_{28} - \Xi_{29} + \Xi_{Q\text{-}1} \text{ (actual and proposed operation)} \quad (4.45)$$

$\dot{\Xi}_L$ and $\dot{\Xi}_D$ are constructed using Equations (3.11) and (3.14). Here, the exergy destroyed along with the flue gases is also taken into account, and the following calculation is done:

$$\sum \Xi_D = \sum \Xi_F - \sum \Xi_p \quad (4.46)$$

Exergy efficiency (ε):

$$\varepsilon = (\sum \Xi_P) / (\sum \Xi_F) \quad (4.47)$$

On the basis of the development potential Equation (3.20), it is written as:

$$\dot{I}_{pot} = \sum \Xi_D (1- \varepsilon) \quad (4.49)$$

Tables 4.25 and 4.26, respectively, demonstrate the streams that are utilised in the whole process at the present and anticipated operations. Table 4.27 displays the exergy of the entire system under actual and suggested operating conditions.

Table 4.25 Main feed and product streams properties of the overall system

Stream No. (Phase)	**1 (Liquid) Actual**	**2 (Vapor) Actual**	**27 (Liquid) Actual**	**1 (Liquid) Proposed**	**2 (Vapor) Proposed**	**27 (Liquid) Proposed**
Total Mass rate ($\dot{m}$) (kg/s)	11.085	8.3333	9.0077	11.085	9.722	9.0521
Temperature (T) (^oC)	60	88	43	60	88	43
Pressure (P) (kPa)	4251.3	3621.0	2471.3	4251.3	3621.	2471.325
Total Molecular wt. (kg/kmol)	109.50	10.972	97.804	109.50	10.972	97.619
Total Enthalpy (H) (MW)	1.5029	4.6922	0.8099	1.5029	4.6922	5.405
Total Sp. Enthalpy (h) (kJ/kg)	135.57	563.06	89.901	135.57	563.06	600.131
Total Sp. Enthalpy at (T_0, P_0) (h_0) (kJ/kg)	60.211	360.32	54.943	60.211	360.32	54.943
Total Sp. Entropy (s) (kJ/kg K)	6.7897	18.120	5.7998	6.7897	18.120	7.013
Total Sp. Entropy at (T_0, P_0) (s_0) (kJ/kg K)	6.5693	20.199	5.6918	6.5693	20.199	5.691
Total Standard API	59.780	421.07	51.401	59.780	421.07	51.401
Sp. Physical Exergy (e^{ph}) (kJ/kg)	9.6475	822.64	545.18	9.6475	822.64	545.188
Sp. Chemical Exergy (e^{ch}) (kJ/kg)	47043.	-26711	46683.	47043.	-26711	46683.49
Physical Exergy ($\dot{\Xi}^{ph}$) (MW)	0.1069	6.855	4.9109	0.1069	6.855	4.910915
Chemical Exergy ($\dot{\Xi}^{ch}$) (MW)	521.49	1799.0	420.51	521.49	1799.0	420.5131

Table 4.26 Off-gas streams properties of the overall system

Stream No. (Phase)	**33 (Vap.) Actual**	**29 (Vap.) Actual**	**28 (Vap.) Actual**	**33 (Vap.) Proposed**	**29 (Vap.) Proposed**	**28 (Vap.) Proposed**
Total Mass rate ($\dot{m}$) (kg/s)	770.694	0.6690	0.3061	770.694	0.6690	0.3061
Temperature (T) (^oC)	1922.23	31.962	31.962	1922.23	31.962	31.962
Pressure (P) (kPa)	901.325	2331.3	2331.3	901.325	2331.3	2331.3
Total Molecular wt. (kg/kmol)	28.2255	42.125	31.262	28.2255	42.125	31.262
Total Enthalpy (H) (MW)	2162.16	0.0601	0.1149	2162.16	0.0601	0.1149
Total Sp. Enthalpy (h) (kJ/kg)	2805.47	89.911	375.43	2805.47	89.911	375.43
Total Sp. Enthalpy at (T_0, P_0) (h_0) (kJ/kg)	97.8944	424.05	410.38	97.8944	424.05	410.38
Totla Sp. Entropy (s) (kJ/kg K)	9.07168	6.8546	8.7870	9.07168	6.8546	8.7870
Total Sp. Entropy at (T_0, P_0) (s_0) (kJ/kg K)	6.19448	8.4397	9.6856	6.19448	8.4397	9.6856
Total Standard API	38.7352	161.93	208.63	38.7352	161.93	208.63
Sp. Physical Exergy (e^{ph}) (kJ/kg)	n/a	-334.1	-34.98	n/a	-334.1	-34.98
Sp. Chemical Exergy (e^{ch}) (kJ/kg)	n/a	33087.51	11858.1	n/a	33087.51	11858.1
Physical Exergy ($\dot{\Xi}^{ph}$) (MW)	n/a	-0.22357	-0.0107	n/a	-0.22357	-0.0107
Chemical Exergy ($\dot{\Xi}^{ch}$) (MW)	2707.57	22.13828	21.37	2707.57	22.13828	21.37

Table 4.27 Exergy of the components for the overall system at actual and proposed operating conditions

	Actual Operation	**Proposed Operation**
Ξ_W (MW)	0.150	0.151
Ξ_2 (MW)	563.06	563.85
$\Xi_{HX\text{-}401}$ (MW)	10.87	10.05
$\Xi_{HX\text{-}402}$ (MW)	10.99	9.09
$\Xi_{F\text{-}401}$ (MW)	9.97	9.45
$\Xi_{Q\text{-}1}$ (MW)	8.90	7.7

The energy and exergy analysis of existing and proposed operations for the entire system are given in Table 4.28.

The overall energy efficiencies of the Reformer unit were determined to be 79% and 81%, respectively, at actual and anticipated operation. The exergy efficiencies were calculated as 25% and 26%, respectively. The corresponding exergy destructions were 41.7 MW and 40.99 MW, while the corresponding development potentials were found to be 4.316 MW and 11.06 MW.

Table 4.28 The energy and exergy analysis of the actual and proposed reformer units

		Act. Operation	**Prop. Operation**
Ξ_P	**(MW)**	4.67	5.32
Ξ_F	**(MW)**	40.96	20.31
Ξ_D	**(MW)**	41.7	40.99
η	**(%)**	79	81
ε	**(%)**	25	26
I_{pot}	**(MW)**	9.316	11.06

4.11 Energy Analysis

It is very necessary to analyze the energy consumed in the process of reformation of naphtha in terms of the economic cost of using fuel for heating operations or the cost of cooling processes used, the AVEVA PRO/II program provides a very useful tool in energy analysis and its economic cost and also provides very good suggestions for energy savings, in this section we have done two very important things: first: analysis of energy consumed in the real plant and energy analysis after the modifications and the second: Proposing processes that reduce energy consumption.

After we applied the modification, we obtained more energy savings given in Table 4.28. We can see from previous tables that after modification, the total required energy is reduced as shown in Table 4.22.

Proposing processes that reduce energy consumption:

Although the process of modifying the conditions has led to a reduction in total energy consumption in the process, there is still the possibility of reducing energy consumption more in other words, the possibility of exploiting hot and cold currents should be sought and thus provide more energy by adding heat exchanger in different scenario or different place, which is as shown in Table 4.29.

Table 4.29 Heat exchanger netework design changes

	Energy Saving [%]	**Payback [year]**	**New Area [m2]**	**Extra Capital Cost ($)**
Case 1	25.26	0.1415	20.06	18,811
Case 2	25.26	0.1415	20.08	18,818
Case 3	0.06	0.3348	48.22	29,798
Case 4	0.06	0.3348	48.21	29,795

From the previous table, we can conclude that the best design suggestion is adding new exchanger case 1 which will save energy by 25.26% and require low capital cost and area compared with other cases.

4.12 Optimum Operation Conditions of Naphtha Reforming

After we studied the effects of available parameters on naphtha reforming, we have to choose the best value which will give as a high value of RON and the values of these parameters are as the following:

1. For the Reformer H_2/HC Ratio we found the best value is 2.6 which gives the highest value of RON 100.31.
2. For the catalyst density, it was found that 640 kg/m^3 of density gives 99.189 RON and at this value the purity of product naphtha is at maximum value.

3. For the feed blend temperature, when temperature increase the RON, aromatics and produced H_2 increase but the mass flow of produced platform ate decreased, so we must choose the value of temperature carefully, the best value is 515^oC which gives 104.5 RON.

4. For Reformer- Product Separator Pressure, when pressure increased the RON, mass flow of H_2 increased while the sum of aromatics and mass flow of reformate decreased so when can consider the value 350 kPas. the best one and will give us 99.69 RON.

5. For Reformer - Catalyst Circulation Rate, when the catalyst circulation rate increase the RON is slightly increase and the unstable naphtha flow rate decreased so this value doesn't have big effect on RON, so the smallest value is good 1200 kg/hr.

We have to mention that we study the effect of only the parameter that we can change in real plant and with constant rest parameter, Table 4.30 show the summary of parameters value.

After we applied the new values of parameters we run the simulation again, and we obtained the result of reactors in new values better than oldest one as shown in Table 4.31.

Table 4.30 Optimum operation conditions of naphtha reforming

Name	**Value**	**Units**
The Reformer H_2/HC Ratio	2.6	------
Catalyst density	640	kg/m^3
Feed blend temperature	515	^oC
Product Separator Pressure	350	kPas.
Catalyst Circulation Rate	30000	kg/hr.

From all previous information, we can see that the software " AVEVA PRO/II " results are validated and we can use it to obtain our target.

Table 4.31 Simulation results comparison of reforming reactors

Result of reactors at **actual operation**		Result of reactors at **proposed operation**
Recycle H_2		**Recycle H_2**
Recycle H_2 Rate [kg/h]	30000	35000
Recycle H_2 Purity	0.70	0.692
H_2 Yield		**H_2 Yield**
H_2 Yield, Wt. [%]	2.61	2.51
Net H_2 Rate [STD_m^3/h]	15402.56	16488.72
H_2 Production [STD_m^3/m^3]	289.671	310.098
H_2 Purity, mole fraction	0.707	0.692
H_2/HC Ratio	1.6	2.511
Yields/RON		**Yields/RON**
C5+ Yield, wt. [%]	85.37	79.02
C5+ Yield, vol [%]	80.39	73.30
C5+ RON	98.53	103.49
C6+ Yield, wt. [%]	80.24	72.23
C6+ Yield, vol [%]	74.60	65.71
C6+ RON	100.36	105.82
Reformate Production [m3/h]	39.712	36.288
Reformate RON	99.67	104.50
Aromatic yields		**Aromatic yields**
Items	Wt.%	Wt.%
Benzene	17.51	19.775
Toluene	12.06	11.573
Ethyl-Benzene	2.013	1.971
Para-xylene	1.641	1.544
Ortho-xylene	2.810	2.693
Meta-xylene	4.679	4.385
Total Xylenes	9.130	8.620
Total Aromatics	49.428	50.18

5. CONCLUSIONS AND RECOMMENDATION

In this thesis, energy and exergy analyses of a catalytic naphtha reforming process were conducted at the Salahuddin I Refinery in Baiji, Iraq. The process was examined and simulated under both actual and proposed operating conditions utilizing the AVEVA Pro/II process simulation program and Microsoft Excel. Based on the simulation data, energy, exergy, and thermoeconomic analyses were performed. Consequently, the energy and exergy efficiencies, exergy destruction, and improvement potentials of the equipment were determined.

The simulation studies were conducted by modifying the operating conditions, specifically by increasing the flow rate of recycled hydrogen (H_2). The flow rate of recycled H_2 was set at 30,000 kg/h for the actual operation and 35,000 kg/h for the proposed operation. Under actual operating conditions, the Research Octane Number (RON) was 99.67, while for the proposed operation, it increased to 104.5 at 515 ^oC reactor temperature. Additionally, the total aromatic content was 49.43% in the actual operation and 50.18% in the proposed operation.

At the conclusion of this research, we recommend the following:

1. Implement the optimized variable values identified in this study, which maximize the octane number while minimizing energy consumption.

2. Integrate an additional heat exchanger to achieve a 25% reduction in energy consumption.

3. Install separation units for light components downstream of the distillation tower to obtain high-value products such as LPG, propane, and various other derivatives.

REFERENCES

Askari, A., Karimi, H., Rahimi, M. R., & Ghanbari, M. 2012. Simulation and modeling of catalytic reforming process. Petroleum & Coal, 54(1): 76-84.

Ancheyta-Juarez, J., Villafuerte-Macias, E., Diaz-Garcia, L. and Gonzalez-Arredondo, E. 2001. Modeling and simulation of four catalytic reactors in series for naphtha reforming. Energy & fuels, 15(4): 887-893.

Antos, G. J., & Aitani, A. M. 2004. Modeling Catalytic Naphtha Reforming. In Catalytic Naphtha Reforming, Revised and Expanded, pp. 519-561, CRC Press.

Antos, G. J., Aitani, A. M., & Parera, J. M. 1995. Catalytic naphtha reforming: science and technology. Marcel Dekker Inc.

Gaggioli, R. A. 1983. Second law analysis for process and energy engineering, In: ACS Publications, Gaggioli, R. A. (eds), American Chemical Society, pp. 3-50, America.

Gary, J. H., Handwerk, J. H., Kaiser, M. J., & Geddes, D. 2019. Petroleum Refining: Technology, Economics, and Markets, Marcel Dekker Inc., pp. 201-210, New York.

Ghasem, N. 2021. Computer methods in chemical engineering. CRC Press. pp. 439-445, New York.

Lai, Y. Q., Manan, Z. A., & Alwi, S. R. W. 2018. Simultaneous diagnosis and retrofit of heat exchanger network via individual process stream mapping. Energy, 155: 1113-1128.

Le Goff, P., Cachot, T., & Rivero, R. 1996. Exergy analysis of distillation processes. Chemical Engineering & Technology: Industrial Chemistry-Plant Equipment-Process Engineering-Biotechnology, 19(6): 478-485.

Liang, K. M., Guo, H. Y., & Pan, S. W. 2005. A study on naphtha catalytic reforming reactor simulation and analysis. Journal of Zhejiang University-Science B, 6(6): 590-596.

Marin, G., & Froment, G. 1989. The development and use of rate equations for catalytic refinery processes. In Studies in Surface Science and Catalysis, 53: 497-511. Elsevier.

Mesa Gómez, A., Valero Valdivieso, M., & Figueredo Medina, M. 2016. Process simulation-based improvements to maximize naphtha production in an existing gas processing plant. Ingeniería y universidad, 20(2): 355-371.

Mohaddecy, S. S., Zahedi, S., Sadighi, S., & Bonyad, H. 2006. Reactor modeling and simulation of catalytic reforming process. Petroleum & Coal, 48(3): 28-35.

Rahimpour, M. R., Jafari, M., & Iranshahi, D. 2013. Progress in catalytic naphtha reforming process: A review. Applied Energy, 109: 79-93.

Shakoor, Z. M. 2013. Optimization of Al-Doura catalytic naphtha reforming process using genetic algorithm. Engineering and Technology Journal, 31(7A): 1276-1296.

Smith, R. 1959. Kinetic analysis of naphtha reforming with platinum catalyst. Chem. Eng. Prog, 55(6): 76-80.

Taskar, U., & Riggs, J. B. 1997. Modeling and optimization of a semiregenerative catalytic naphtha reformer. AIChE Journal, 43(3): 740-753.

Tsatsaronis, G. 2008. Recent developments in exergy analysis and exergoeconomics. International Journal of Exergy, 5(5-6): 489-499.

Van Gool, W. 1992. Exergy analysis of industrial processes. Energy, 17(8): 791-803.

Vashishtha, S., Sharma, S., Pal, P., & Maheshwari, U. 2013. Modeling, Simulation and Optimization of Naphtha reforming process on ASPEN Plus platform. Chemcon 2013 66th Annual Session of Indian Institute of Chemical Engineers, 1-5, Mumbai.

Worrell, E., & Galitsky, C. 2005. Energy efficiency improvement and cost saving opportunities for petroleum refineries. U.S. Department of Energy, 105 p., Berkeley.

Wu, Y.-y., Li, W., Xu, Y., Jin, E.-h., & Tu, Y.-y. 2011. Evaluation of the antioxidant effects of four main theaflavin derivatives through chemiluminescence and DNA damage analyses. Journal of Zhejiang University Science B, 12: 744-751.

Zakari, A., Aderemi, B., Patel, R., & Mujtaba, I. M. 2019. Study of industrial naphtha catalytic reforming reactions via modelling and simulation. Processes, 7(4):192.

CURRICULUM VITAE

Personal Information

Name and Surname : Taha Asheooe Issa ISSA

Education

M.Sc.	Çankırı Karatekin University Graduate School of Natural and Applied Sciences Department of Chemical Engineering	2020-Present
Undergraduate	Tikrit University Department of Chemical Engineering	1997-2003

Work Experience

Year	**Institution**	**Position**
2005-2007	Northern Fertilizers Company / Baiji	Engineer
2007-Present	Ministry of Oil/Iraq- North refineries Company / Baiji	Senior Chief Eng.